Materials Advances

ROYAL SOCIETY OF CHEMISTRY

REVIEW

View Article Online
View Journal | View Issue



Cite this: *Mater. Adv.*, 2025, 6, 887

# A review on mechanical metamaterials and additive manufacturing techniques for biomedical applications

Suhas P.,[a] Jaimon Dennis Quadros,[b] Yakub Iqbal Mogul,[c] Ma Mohin,[d] Abdul Aabid, *[e] Muneer Baig[e] and Omar Shabbir Ahmed[e]

Received 1st September 2024,
Accepted 9th December 2024

DOI: 10.1039/d4ma00874j

rsc.li/materials-advances

This review presents the design and experimental analysis of metamaterials with tunable properties for biomedical applications. Five different metamaterials, such as lightweight metamaterials, pattern transformation metamaterials, negative compressibility metamaterials, pentamode metamaterials and auxetic metamaterials, are discussed in detail with emphasis on their mechanical and biological features that are primarily applicable in the field of biomedical technology. Various indigenous structures of the metamaterials are carefully analysed for metamaterial design and their influence on mechanical performance is studied. Thus, this review comprehensively summarizes the different additive manufacturing techniques implemented for biomedical metamaterials and their influence on their mechanical properties. Finally, the mechanical properties and deformation mechanisms for different geometries and structures of all the above-mentioned metamaterials are analyzed.



## 1 Introduction

Metamaterials are artificial materials exhibiting properties that are not present in naturally occurring materials. Recently, there has been a surge in the popularity of metamaterials owing to their potential applications in several industries.[1] Metamaterials exhibit a diverse set of mechanical and biological characteristics that are applicable in biomedical engineering.[1,2] There are a few regulatory challenges in the incorporation of metamaterials for biomedical applications, which include avoiding adverse reactions with bodily fluids, requiring long-term stability, maintaining sterile standards and manufacturing consistency, and interaction with biological parts.[2,3] Conducting a thorough examination of the mechanical and biological features of metamaterials is necessary for the researchers to acquire a comprehensive understanding of the potential applications of these materials in the field of biomedical engineering.

The development of vascular stents and bone implants is one area of metamaterial research with biological applications.[3] These devices are primarily used in the treatment of cardiovascular disorders and bone abnormalities. To effectively incorporate such devices into the human body, it is necessary to choose materials that possess appropriate biological and mechanical characteristics. Metamaterials, with their diverse microstructure and enhanced mechanical characteristics, have great potential for enhancing the performance and lifetime of vascular stents and bone implants. Moreover, in biomedical engineering, the capacity to differentiate amid the mechanical properties of metamaterials is quite beneficial. Shape memory polymers, known for their great elasticity and ability to adapt to numerous bodily conditions, are commonly utilised in the fabrication of vascular stents.[4,5] This flexibility is vital for attaining optimum performance while accommodating potential obstacles. Because of their mechanical and biological properties, metamaterials have been used widely in biomedical engineering, which has sparked increased interest in further studies.[6] The remarkable properties of metamaterials and their probable applications in biomedical engineering, particularly in the development of novel implants and medical devices, are prudently explored in this review.

Metamaterials can be engineered to perform the mechanical properties of natural bone, which will improve support and biocompatibility.[3,7] According to several studies, this has the potential to transform the field of bone implants.[8] Likewise, the

[a] *Department of Mechanical Engineering, Sahyadri College of Engineering and Management (Visvesvaraya Technological University), Mangalore, 575007, India. E-mail: suhas.me@sahyadri.edu.in*
[b] *Department of Mechanical Engineering, University of Bolton, RAK Academic Center, 16038 Ras Al Khaimah, United Arab Emirates. E-mail: j.quadros@bolton.ac.uk*
[c] *National Center for Motorsport Engineering, University of Bolton, Deane Road, Bolton, BL3 5AB, UK. E-mail: y.mogul@bolton.ac.uk*
[d] *Department of Mechanical Engineering, School of Engineering, University of Bolton, Deane Road, Bolton BL3 5AB, UK. E-mail: m.mohin@bolton.ac.uk*
[e] *Department of Engineering Management, College of Engineering, Prince Sultan University, PO BOX 66833, Riyadh 11586, Saudi Arabia. E-mail: aaabid@psu.edu.sa, mbaig@psu.edu.sa, oahmed@psu.edu.sa*

flexible porosity and permeability of these materials help to speed up healing and reduce the chance of implant rejection by allowing improved absorption into surrounding tissues.[9,10] By leveraging their exclusive mechanical characteristics, such as shape memory and customizable stiffness, metamaterial-based stents can respond to varying blood flow conditions and lower the risk of restenosis.[11] Additionally, because of their bioactive properties, some metamaterials can encourage endothelialization, plummeting the danger of thrombosis and increasing long-term vascular health.

With importance to their mechanical and biological features that make them excellent for applications, the review will look at five different types of metamaterials: auxetic metamaterials, pentamode materials, negative compressibility metamaterials, pattern transformation metamaterials, and lightweight metamaterials. The review will also highlight significant data on the additive manufacturing techniques employed to develop these metamaterials, looking at the likely problems and potential involved in including metamaterials into biological equipment, providing insights into the field's forthcoming directions.

## 2 Biomedical metamaterials

Biomedical metamaterials have exceptional mechanical properties that make them ideal for special applications. Mechanical metamaterials have superior mechanical performances, *e.g.*, negative Poisson's ratio (NPR), negative elasticity, negative compressibility, thermal conductivity, tunable stiffness, and energy absorption, which are used for different applications, as shown in Fig. 1. The classification is grounded on the Young's modulus ($E$), shear modulus ($G$), bulk modulus ($K$), Poisson's ratio ($\upsilon$), and mass density ($\rho$) of mechanical metamaterials[12–14] For example, lightweight metamaterials are beneficial for bone implant applications as they can lower the weight while sustaining sufficient strength and durability.[14] In vascular stents, the tunable stiffness and shape memory properties of metamaterials allow for self-expansion in specific locations, facilitating drug distribution structures and improving blood movement.[3] Additionally, auxetic metamaterials can be used in vascular stents to increase the vessel coverage and offer better resistance forces, avoiding vessel occlusion and narrowing.[15,16] Overall, biomedical metamaterials play a critical role in improving the working and functionality of various biomedical devices, such as vascular stents, bone implants, and artificial organs. These materials allow for tailored design and functionality, enhancing the performance and functionality of biomedical devices.[17] However, not all types of metamaterials are appropriate for biomedical applications. It should be noted that the mechanical properties of metamaterials used in biomedical applications are crucial considerations. Therefore, the

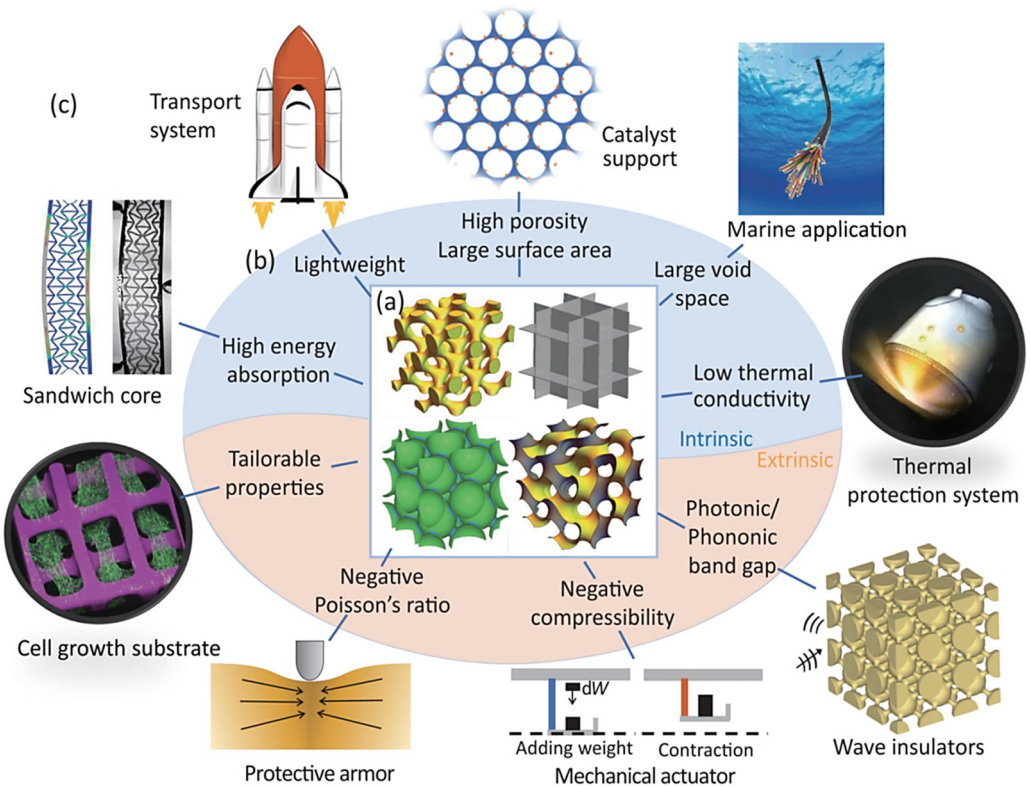


Fig. 1 Mechanical metamaterials with various properties and applications, including energy absorption and lightweight structure, and unique characteristics, like negative Poisson's ratio and negative compressibility. Metamaterial applications in diverse fields, such as aerospace and marine, are displayed owing to their mechanical and thermal attributes. This figure was modified from the originals and reprinted with permission from Jia *et al.*[2] Copyright 2020 the American Institute of Physics.

current section discusses the various metamaterials specifically used for biomedical applications.

### 2.1 Lightweight metamaterials

Lightweight metamaterials with high stiffness are developed by fine-tuning the stage network topology of biphasic or cellular materials. The four forms of mechanical metamaterials are distinguished by their distinct mechanical properties at the macro level, which are created by modifying the microstructure. Table 1 lists the lightweight mechanical metamaterials, each with unique properties and potential biological applications. Such lightweight metamaterials are classified into four types depending on their framework: micro/nanolattice metamaterials, chiral metamaterials, origami-inspired metamaterials, and cellular origami metamaterials.

Micro-/nanolattice metamaterials are made up of various intervallic preparations of unit cells that may be built as beam-based, plate-based, or minimum surface-based structures,[22] as shown in Table 1. By controlling the microscopic topology, the appropriate large-scale mechanical characteristics are accomplished, making them useful in a variety of applications. Several investigators developed micro/nanolattice materials with densities that are lower than that of water, like foam, but with the stiffness and strength of steel.[23–25] For example, a large-area multifunctional metal nanolattice was built with an ultra-high tensile strength of 257 MPa, making it 2.6 times tougher than prior porous materials, but having a relative density of just 0.298.[26] Although these metamaterials possess excellent mechanical properties, they tend to invariably underperform under cyclic loading and extreme temperatures, thereby making their use limited under such conditions.[24]

Chiral materials are another type of lightweight metamaterials that have non-overlapping mirror images and are classified as left- or right-handed (refer to Table 1). Prall and Lakes[27] became the first to develop a hexagonal honeycomb chiral material using Wojciechowski's hypothesis.[28] The unit cell is made up of six ligaments interconnected by axisymmetric rotation about a central cylinder that serves as a node. Table 1 illustrates the anti-chiral structures, in which consecutive nodes of the basic unit are linked on the opposing adjacent of the ligament. Chiral structures, particularly anti-chiral structures, compress and expand ligaments surrounding nodes under compression and tensile loads, resulting in materials with a NPR, or auxeticity. Many researchers have utilized chiral structures to develop 2D and 3D metamaterials that have substantial adaptable ratios and ultrafast shape restructuring reactions, leveraging prestressed shells' bistability and energy conversion features to accomplish spontaneous shape reconfiguration.[18] However, these metamaterials have some issues with regard to the manufacturability and cost, and as a result, its design and production could be technically challenging at a microscopic scale.[19] Hierarchical structures, unlike

Table 1 Lightweight metamaterials of different types

| Types | Examples | Features | Ref. |
|---|---|---|---|
| Nano-lattice metamaterials | 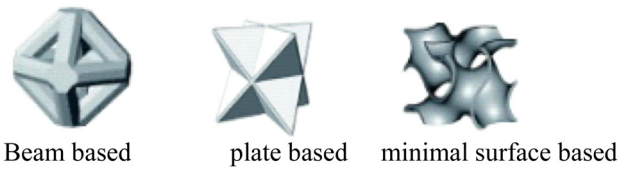  | High strength and stiffness | This figure was modified and reprinted with permission from Lu *et al.*[18] Copyright 2022 ScienceDirect.com by Elsevier. |
| Chiral and anti-chiral metamaterials | 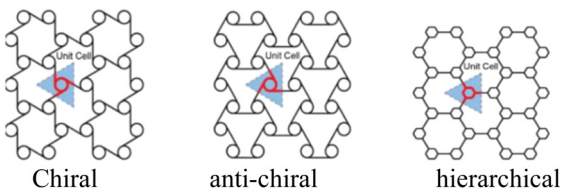  | Bistability, deployable ratios, and ultrafast shape configuration responses | This figure was modified and reprinted with permission from Mousanezhad *et al.*[19] Copyright 2016 ScienceDirect.com by Elsevier. |
| Origami inspired metamaterials | 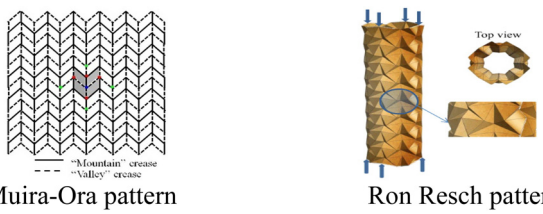  | Flexible, compact, and deformable | This figure was modified and reprinted with permission from Lv *et al.*[20] Copyright 2014 Nature Portfolio. |
| Cellular origami metamaterials | 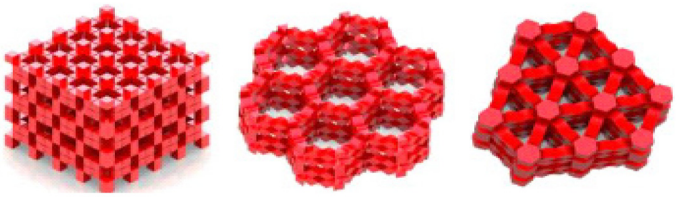  | Deployable, tunable Poisson's ratio, and interfacial surface area | This figure was reprinted with permission from Yang and You[21] Copyright 2020 arxiv.org |

chiral or anti-chiral structures, feature square, rhombic, or polygonal nodes with increased stiffness.[19] See Table 1 for details.

Origami, taken from Japanese, is a conventional form of portable paper in Japan. Origami's intricate and varied folds enable the creation of attractive three-dimensional structures,[29] as demonstrated in Table 1. Several lightweight metamaterials based on origami patterns have emerged: the Miuraori pattern[20] and the nonperiodic Ron Resch pattern[29] to name a few. They are adaptable, malleable, and lightweight. Han *et al.*[30] suggested an origami-based mechanical memory metamaterial, which might effectively reduce oscillations by swapping between memories.

Cellular origami lightweight metamaterials use origami design concepts to make 3D cellular materials, creating foldable structures. It combines origami structure with micro/nanolattice layout. Table 1 displays the two types of cellular origami metamaterials: stacked and interlaced,[31–33] a novel category of origami cellular metamaterials with variable Poisson's ratio (PR). Cheung *et al.*[32] describes origami interleaved tube cellular materials, which have a large interfacial surface area and may be deployed.

Lightweight metamaterials exhibit properties such as strength-to-weight ratios *via* lattice structures such as micro/nano and origami patterns. Designs in terms of novel mechanical structures include the hierarchical and fractal designs that offer unprecedented strength while remaining lightweight. These metamaterials are highly innovative; however, they require precision manufacturing to avoid defective tolerance and prevent mechanical degradation.[20,29] Moreover, these metamaterials are mechanically complex and develop flaws during precision machining, affecting the consistency and reliability in load-bearing applications. Unlike these designs, the conventional ones are more focused on a high load bearing capacity with minimal weight rather than dynamic adaptability.

### 2.2 Pattern transformation metamaterials

Mechanical metamaterials use variable stiffness to modify patterns. When a material reaches a particular deformation threshold, its internal structure changes, resulting in a macroscopic phase shift and adjustable stiffness. This metamaterial enables a phase transformation between microstructures. Tomohiro[29] found that external stress may cause patterns to shift across the metamaterial. To differentiate between pattern transformation and additional metamaterials, it is important to consider auxetic materials with an NPR. Compression alters the stiffness of the design alteration metamaterial in both longitudinal and normal directions. As a result, the material's PR varies with unclear positive and negative signs, and it differs for auxetic metamaterials, which have a set NPRs.[33,34] It is important to differentiate between chiral/anti-chiral metamaterials and adjustable stiffness from pattern transformation. The pattern transformation's adjustable stiffness depends on the configuration and arrangement of holes in the topology. The holes are of conventional forms (circles, ovals, and polygons) or irregular shapes (see Fig. 2). Mechanical metamaterials may be optimized for topology by adjusting their hole form.[21,35] Overveiled and Bertoldi[36] describe the structural stress–strain response as a measure of the progressive stiffness of a structure following hole optimization. As compressive strain develops, the very first linear elastic stiffness phase occurs, followed by nearly negligible incremental stiffness. Lastly, stiffness rises dramatically when the hole collapses.

Hole arrays are classified into four types: square, triangular, trihexagonal, and rhombitrihexagonal. Hole arrays of various dimensions can be used for optimizing the topology in pattern

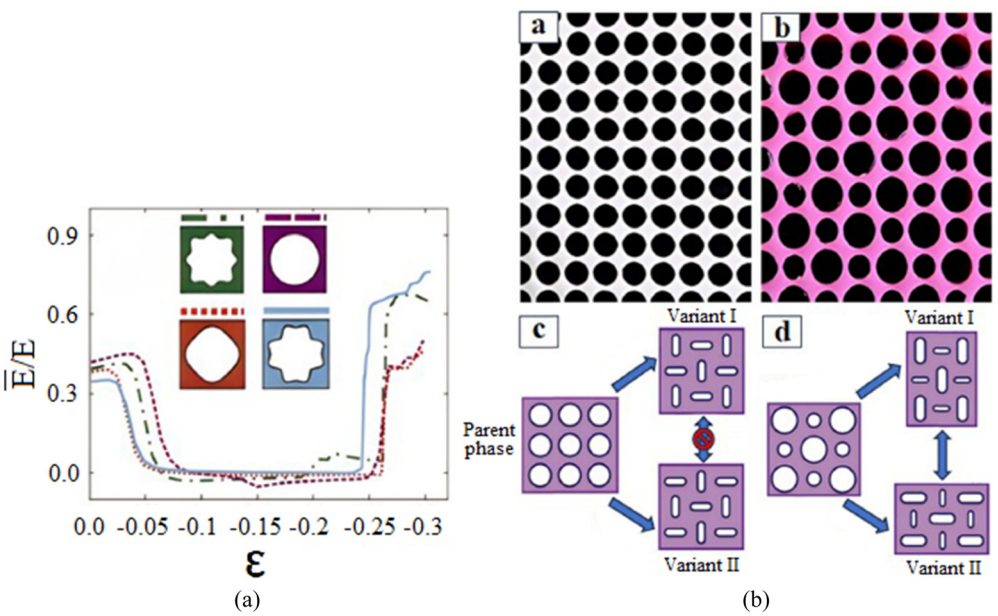


Fig. 2 Pattern changes with variable stiffness. (a) Hole shapes. (b) Array of holes: (a) holey sheets. (b) Biholar sheets. (c) Phase transitions for holey sheets. (d) Phase transitions for biholar sheets.[37] This figure was reprinted with permission from Wang *et al.*[37] Copyright 2023 Frontiers Media SA.

transformation. According to Bertoldi *et al.*[38] and Florijn *et al.*,[39] holey sheets have an identical hole size, but biholar sheets have two distinct sizes of circular holes, as illustrated in Fig. (2b). The holey sheet resembles a periodic elastomeric micro-lattice structure composed of beams. The framework's nonlinear stress–strain pattern offers greater energy absorption. According to Bertoldi *et al.*,[38] the material's nonlinear stress–strain pattern following compressive loading can be attributed to the linear responsiveness of the stress generated by early structural instability in the microstructure. Buckling in cellular microstructures causes localized deformation *via* the collapse band during continual load, leading to significant strain.[40] The biholar sheet is like a customizable mechanical metamaterial with an NPR. Florijn *et al.*[39] reported that the biholar mechanical metamaterial causes nonlinear deformation coupling in both major axes, breaking the symmetry. Yang *et al.*[41] noticed that reversible elastic instabilities can cause pattern changes and allow for switching between different forms. The pattern transformation allows for customizable stiffness and NPR. Cao *et al.*[42] states that the buckling mode is activated by a serious effective threshold and an NPR due to pattern transformation. Tan *et al.*[43] established a real-time controllable negative stiffness mechanical metamaterial, presenting multistage pattern modification to achieve high vibration isolation and energy absorption efficiencies. Metamaterials that exploit the mechanically unstable nature of periodic porous elastic structures hold potential for several applications.

Pattern transformation metamaterials have sparked extensive consideration due to their amazing potential to adjust electromagnetic waves, acoustic waves, and mechanical vibrations. While these metamaterials provide excellent applications for smart systems, their performance is largely affected by sensitive environmental conditions that limit their stability and predictability.[43] This can be improved by enhancing the material robustness, environmental tolerance, and cost-effective manufacturing. The unique designs of pattern transformation metamaterials come with their ability to reconfigure their internal structures under loading conditions that include mechanical and thermal stresses.[41] Such materials use stable structures at different levels that undergo major, reversible deformations. In comparison to the other metamaterials, these metamaterials having fixed lattice structures possess a dynamic structure that adapts to changes in environmental conditions. This ability is largely dependent on the material activation mechanisms that tend to restrict their reliability when they are used in varying or uncontrollable conditions.[42] These materials offer exclusive options for a wide range of biological applications including imaging, sensing, treatment, and drug administration. The enormous utilities of pattern transformation metamaterials in biomedicine are detailed in the sections to follow.

### 2.3 Negative compressibility metamaterials (NCMs)

Negative compressibility, or negative bulk modulus, occurs when a material extends under compression and shrinks under tension.[37] Compressibility, an indicator of a solid or fluid's volume change in reaction to pressure modifications, is often positive.[44] Negative compressibility has a unique effect whenever a system transitions from a stable to a metastable state due to force.[45] Metamaterials with negative compressibility are divided into three types: negative linear compressibility (NLC), negative area compressibility (NAC), and negative thermal expansion (NTE), as shown in Fig. 3.

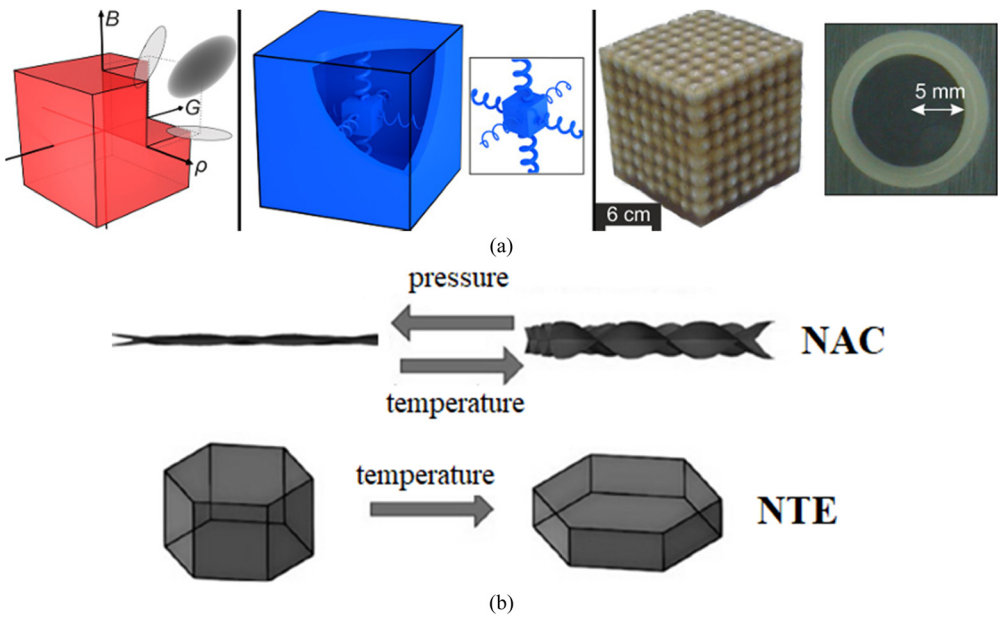


Fig. 3 (a) NCM with stress application in principal directions: (left) 3D unit-cell geometrical arrangement of the NCM (middle), cross-sectional view of the metamaterials. (b) Negative compressibility metamaterials (NCMs) exhibit unique responses to temperature and pressure changes. NCMs under pressure expand (NAC) and contract upon cooling (NTE), exhibiting counterintuitive behaviors.[43] These figures were modified and reprinted with permission from Wang *et al.*[43] Copyright 2023 Frontiers Media SA.

NLC is a unique material feature where a system grows in a single direction when evenly compressed.[46] NLC materials encompass both natural and synthetic materials. Natural materials with low negative compressibility include *R*-cristobalite-structured $BAsO_4$ and KMn $[Ag(CN)_2]_3$.[47] These materials exhibit a somewhat mild NLC effect. Artificial materials using a structure with a wine-rack, honeycomb, or analogous topology can achieve greater values of negative compressibility. Li *et al.*[48] created a 3D hybridized zinc formate structure with NLC using metal–organic frameworks (MOFs), $[NH_4][Zn(HCOO)_3]$. Ghaedizadeh *et al.*[49] offered two methodologies for developing and fabricating innovative composite structures with NLC. The experimental findings reveal that the suggested material structures have NLC features because of the compressibility of the foam filler, the position of network parts, and the stiffness ratio amongst the two materials.

NAC, or enlargement of compressed crystals in either direction, is unusual or weaker than NLC.[50] Densification in multilayer materials often commences with stacking direction compression, followed by extensions in both perpendicular directions inside the layer.[51] When exposed to hydrostatic compression, the molecular structure of Ag (tcm) (where tcm stands for tricyclic methanation) continually develops in two orthogonal directions. The disintegration of interlayer gaps causes the honeycomb-like portions to flatten fast, resulting in negative area compressibility.[51]

NTE is the compression of a material upon heating.[51,52] NTE metamaterials conserve energy, yet when heated up, they shrink in various directions rather than expanding.[35] Cairns *et al.*[47] found a relationship among anisotropic NTE and NLC/NAC in structure materials. Anisotropic NTE characteristic is also a form of negative compressibility. Researchers have used the unique feature of negative compressibility for technological purposes. Tortora *et al.*[53] created a metal–organic framework (MOF) by placing a non-wetting liquid in an elastic porous substrate with a high negative compressibility. Kim *et al.*[54] developed a broadband muffler using a metamaterial made up of a membrane framework with negative density and a Helmholtz resonator with negative functional compressibility. This resulted in a specific metamaterial muffler with a broad working frequency spectrum. Mechanical metamaterials with negative compressibility have a possible application in engineering to satisfy requirements. These types of metamaterials face significant constraints due to operational range and complex structures. This cost and complexity restrict its ability for scalable manufacturing and widespread use. The development of robust materials and simplified structures maintain such materials across a wide range of stress and environmental conditions.[45] NCMs exhibit varying geometries in their structural designs during compression. This is primarily achieved through internal structures, namely chiral geometries, or frameworks with interlocking components.[51,52] During compression, NCMs with the negative compressibility characteristic possess the ability to absorb significant energy and become shock resistant, developing their suitability for protective applications. This negative compressibility is achieved through interactions with complex internal networks, as they are specifically designed to expand under compressive forces.[52] Due to their structural complexity, NCMs are susceptible to material fatigue, especially under cyclic loading.[44]

### 2.4 Pentamode materials

Pentamode metamaterials are typically characterized by their unique ability to exhibit fluid-like behaviors without deterring their solid structure[55] shown in Fig. 4. These materials comprise specific diamond shaped lattice structures/geometries that resist compression in one direction, offering minimal shearing resistance in the other directions.[55–57] By modifying the diameter dimensions, the creation of pentamode metamaterials with diverse architectures can be enabled. Efficient topology optimization approaches can reveal new pentamode lattice microstructures with diverse material characteristics.[58] Furthermore, efficient wave manipulation of pentamode metamaterials may be realized underwater at frequencies less than 1000 Hz.[59] Pentamode metamaterials are currently being utilized to tackle difficulties in a variety of industries because of their distinct mechanical features.

### 2.5 Auxetic materials

Auxetic metamaterials, or NPR materials, contract laterally when compressed and expand laterally when stretched,[22] and are classified as chiral structures, rotating stiff structures, re-entrant structures, and perforated sheet structures.[34] While ordinary honeycomb structures lack auxeticity, Table 2 shows

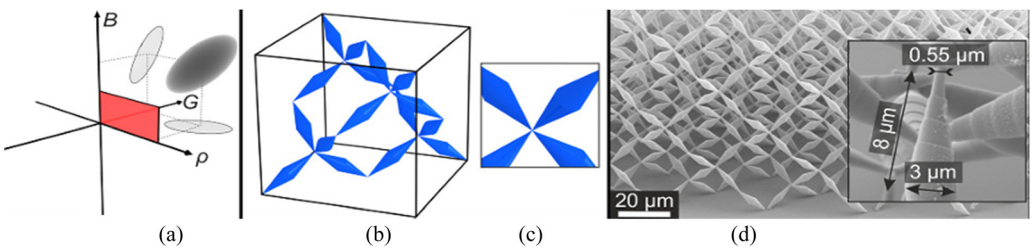


Fig. 4 Pentamode metamaterials exhibit fluid-like behavior under stress conditions, retaining a solid framework. (a) Pentamode metamaterial stress application in principal directions, (b) 3D unit cell geometrical arrangement of the pentamode metamaterial, (c) 2D representation of the 3D unit cell, and (d) the macroscopic view of the lattice structure. This figure was reprinted with permission from Christensen *et al.*[55] Copyright 2015 Materials Research Society.

that re-entrant hexagonal honeycombs have this attribute. When stretched longitudinally at each end, the re-entrant hexagonal honeycomb structure expands transversely (NPR), whereas the typical honeycomb structure contracts transversely (positive Poisson's ratio).[22] Several distinct geometric structures including auxetic arrowhead structures[60] have been demonstrated to have re-entrant mechanisms in addition to the re-entrant hexagonal honeycomb structure. Furthermore, Yang *et al.*[61] state that 2D structures may be employed to create 3D re-entrant structures. As technology for additive manufacturing advances, it will be possible to create 3D re-entrant structures to address problems. Using the electron beam melting method, Yang *et al.*[61] created and produced a Ti–6Al–4V 3D re-entrant lattice auxetic structure. The outcomes demonstrated that this structure outperforms traditional materials in terms of mechanical efficiency.

Table 2 shows that chiral structures, as discussed in Section 2.1, exhibit NPR. Mechanical forces causes the cylinder to spin, enabling ligaments to flex and unfold or fold depending on tensile or compressive loading. Therefore, these structures exhibit auxetic properties. Introducing cylinders in chiral honeycomb shapes reduces rigidity compared to re-entrant hexagonal honeycombs.[63] Anti-chiral honeycombs have reduced moduli compared to chiral equivalents with a comparable number of ligaments.[64] Creating periodic chiral structures requires adhering to the symmetry of rotation. There are however just five structural types: trichirals, anti-trichirals, tetrachirals, antitetrachirals, and hexachirals. According to C.-X. Lu *et al.*,[22] Poisson's ratio of chiral structures is impacted by both the ratio of ligament or cylinder wall thickness to cylinder radius and the ratio of ligament length to cylinder radius. *meta*-Chiral designs lack rotational symmetry and use both chiral and anti-chiral features to improve auxetic behavior. A *meta*-tetrachiral configuration combines tetrachiral and anti-tetrachiral structures, changing its nodes from cylindrical to rectangular.[62] This *meta*-tetrachiral structure has a Poisson's ratio of much less than −1.0. Nevertheless, an NPR is only possible with modest stresses. Rotating structures often consist of standardized geometric forms linked by hinges, as shown in Table 2. These geometrical forms contain squares, rectangles, triangles, rhombuses, and parallelograms. When mechanically loaded, the stiff structure revolves around its hinge point. It

Table 2 Different types of auxetic metamaterials

| Types | Examples | Features | Ref. |
|---|---|---|---|
| Re-entrant structures | 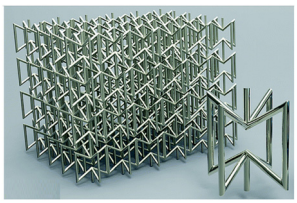 | The thermodynamic requirements call for a big negative Poisson's ratio and high stiffness. | This figure was modified and reprinted with permission from Kolken and Zadpoor *et al.*[34] Copyright 2017 Royal Society of Chemistry. |
| Chiral and anti-chiral structures | 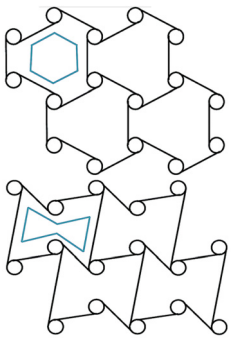 | Consistent Poisson's ratio over several strains and high deployability ratios. | This figure was modified and reprinted with permission from Alderson *et al.*[35] Copyright 2010 ScienceDirect.com by Elsevier. |
| Rotating structures |  | A varied variety of Poisson's ratios (negative to positive). | This figure was modified and reprinted with permission from Grima *et al.*[62] Copyright 2008 Wiley Online Library. |
| Perforated sheet structures | 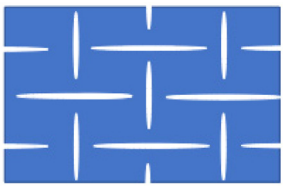 | Easy production procedure, a small range negative. | This figure was reprinted with permission from Tang *et al.*[15] Copyright 2020 American Ceramic Society. |

expands under unilateral tension and collapses under unilateral compression. Rotating rectangular structures are formed by substituting squares with rectangles. They are classified into two varieties based on the geometry of the vacant area. According to Grima *et al.*,[62] the unoccupied area of type I is shaped like a rhombi, with the Poisson's ratio varying from negative to positive. The unoccupied area of type II is shaped like a parallelogram, with processes comparable to spinning square structures.[65,66] However, the connection differs. Research has found that Poisson's ratios of spinning rhombic and parallelogram constructions vary based on loading orientation, geometry, and unoccupied area.[67–69]

Grima and Gatt[70] discovered that perforated sheet constructions with varying designs of standard blocks or sheets result in combinations with a NPR, as shown in Table 2. They observed that diamonds and star perforated sheet structures exhibit an NPR in both compression and tension, which explains its auxetic behavior. They also discovered that perforated sheet structures are easier to make compared to other auxetic structures, despite their similarity to rotating ones. Perforated sheet constructions were often restricted in their ability to display NPRs. Mizzi *et al.*[71] presented an array of extremely anisotropic auxetic perforated metamaterials with excellent tunability and the possibility for a wide range of Poisson ratios. Artificial intelligence models now allow for faster and more accurate construction of auxetic perforated sheet metamaterials.[72] Despite the significant potential of auxetic metamaterials for energy absorption, they face several limitations, including low elastic modulus, low strength, high cost, and inefficient fabrication processes.[70]

In addition to auxetic metamaterials, several structures have NPRs. Microporous polymers, which include PTFE, exhibit auxetic activity.[73,74] PTFE has considerable anisotropy, exhibiting a Poisson's ratio as low as −12.0. Origami metamaterials (described in Section 2.1) also exhibit NPR. The Miura origami pattern may attain NPR with proper design specifications.[75] The re-entrant and chiral structures of the auxetic metamaterials expand laterally when they are stretched, thereby achieving their negative Poisson's ratio, which enhances the mechanical properties such as impact strength and shear strength, making them viable for biomedical applications.[22] This auxetic response is quite different from other metamaterials as these structures densify when subjected to tension, ensuring uniform distribution of force. These structures, however, pose challenges during fabrication due to their complex geometries limiting their reliability under extreme conditions.[61] Mechanical metamaterials may be classified using several criteria and methods. Table 2 summarizes the many forms of auxetic mechanical metamaterials.

# 3 Application of metamaterials in the biomedical field

## 3.1 Biomechanical engineering

A compliant material is an NPR-like chiral material that gets thicker on stretching unlike the usual materials that get thinner when stretched.[76] In biomedical engineering, they can be employed to create stents and scaffold necessary in the tissue engineering.[76] Along the same line, aerogels, thus, also belong to the class of materials which are lightweight, low density and highly porous in nature. These are for drug delivery systems, wound healing systems and femoral tissue systems. The composite system offers a large external surface area than the other controlled drug delivery systems and can be modified/control the release of the drug.[77] Using auxetic materials, joint replacements and bone transplants are some of the orthopedic implants that can be done. It can be used in building stents with relatively flexible construction that is suitable to be inserted in arteries. It also reveals that the materials expand more consistently, hence lowering impacts on the tissues and increasing blood flow.[78]

## 3.2 Imaging, sensing and diagnostics

Metamaterials are light in weight and this property when integrated in structure with biological systems, for instance, with molecular and cellular systems will provide very highly sensitive and accurate information, which will assist us to understand the processes of complicated diseases and illnesses. It must also be noted that transforming pattern metamaterials lead to the formation of the non-conventional imaging system with high resolution and sensitivity. The pentamode materials have the potential to work as the contrast agents or the probes in the biomechanical imaging techniques such as elastography and shear wave imaging.[79] These probes based on metamaterial can create mechanical waves or alter the tissue's elasticity and offer a broad range of information regarding the tissue mechanical properties on any disease-related anomaly such as cancer or fibrosis.[79] Benefiting from the reversible transition between monomodal and pentamode, possible selective catch-molecules or receptors can be anchored to the surface, in which the target molecules of concern selectively interact with the catch-molecules and in turn, get a measurable mechanical signal. Based on the discussed different deformation characteristics of auxetic materials, the latter are widely used to create effective strain and pressure sensors. In as much as they can be incorporated on wearable equipment as far as monitoring is concerned, and in as much as one's health status is of concern, this is all true. In essence, this kind of metamaterials can be used to improve imaging devices such as MRI and ultrasounds. They can be flexed to conform to the movements of the body, shape, and they have skin contact; therefore, it is possible to have better and enhanced shots.[78,80]

## 3.3 Therapeutic devices

Metafluids are light thermofluids for which the new design parameters are associated with the changed microstructure. In the drug delivery application, Metamaterial can be embedded to design drug delivery systems which have high sensitivity of pressure. The fabrication of personal mechanical properties of metamaterial-based braces, supports or orthoses for restoration of functionality or orthopedic appliances allow better support and stability, alignment of the involved joints or

tissues and thus relief from pain, enhanced mobility and rehabilitation.[6] An additional aspect familiar with the supporters of auxetic characteristics is their application in bone grafts and prosthetic implants as significant compatibility with the tissues, which, in turn, has positive effects on certain surgical interventions' symptoms.[81] In assistive devices such as exoskeletons or other supportive frameworks, auxetic materials give contour adaptability that can effortlessly shift in synchrony with the user's movements.[82]

### 3.4 Wearable and implantable devices

Hierarchical honeycomb structures (HHS) are periodic structures with honeycomb cells, created at different scales and then arranged in such a way that they have a repetitive feature. Metamaterials with negative compressibility will have practical relevance in biomedical equipment, including vascular stents and orthopedic implantation equipment. These materials can improve the interaction with the overlying and/or surrounding tissues and reduce the probability of inflammation; furthermore, they possess satisfactory mechanical properties for withstanding physiological pressure.[83]

### 3.5 Drug delivery systems

Aerogels are a kind of material that is highly porous with very low density and thus very light. Some of these are in the use of taking drugs, in dressing of injuries, and acting as a support structure for tissues. These are also foldable structures inspired by origami and hence can be easily used for minimal invasive medical instruments or even surgical instruments. In the field of biomedicine, it can be applied for endoscopic instruments, catheters, and drug delivery systems. Their small and portable design makes it possible to locate them in areas within the body that may be difficult to access and, at the same time, the tissue damage is reduced.[84] To summarize, it can be stated that the delivery mechanisms of drugs may contain elements with certain features within the external environment (light, temperature, magnetic field, *etc.*) that will allow you to coordinate the process of drug release by space-time accurately. To the best of authors' knowledge, the application of negative compressibility metamaterials has not been discussed in recent studies; however, if applied in drug delivery use, they can form delicate drug carriers.[44] When those materials are compounded with nanoparticles or hydrogels, one can create systems that could actively increase in size upon exposure to certain factors such as temperature change or changes in pH level, thereby enabling the targeted and controlled release of the therapeutic drug in the right part of the human body.[37,44] Application of Pentamode-based drug distribution systems are in cancer therapies, chronic disease control, regenerative medicine among others. Auxetic materials are utilized in the systems that transport drugs to tissues in the body. This is precisely useful for handling localized issues like tumors or infections. Auxetic materials improve medication delivery and retention in joint areas, ensuring improved therapeutic efficiency for illnesses such as arthritis.[78] A complete utilization of metamaterials in drug distribution has been represented in Fig. 5.

## 4 Additive manufacturing of biomedical metamaterials

Biomedical metamaterials have specific mechanical characteristics determined by their geometry, such as micro/nano lattice architecture, rather than composition.[84–86] Mechanical metamaterials may be customized to provide various mechanical characteristics.[87] They involve elastic modulus, strength, Poisson's ratio, recoverability, and energy absorption. Biomedical metamaterials including auxetic,[88–92] pentamode,[93] lattice structure,[94] and lightweight metamaterials[95] are being intensively explored. Additive manufacturing (AM) technologies are a feasible choice for fabricating mechanical metamaterials because of their capacity to create high-resolution 3D structures utilizing computer-aided design (CAD) files and independently customize design unit cells. The summary covers the furthermost predominant additive manufacturing technologies utilized to lightweight, pattern transformation, negative compressibility, pentamode, and auxetic metamaterials.

### 4.1 Vat polymerization

Vat polymerization is a prevalent method for manufacturing biomedical metamaterials *via* AM. These methods are extensively employed to produce advanced metamaterials such auxetic and pentamode structures.[96,97] Buckmann *et al.*[97] formed auxetic metamaterial frameworks with sub-micron unit cells using multi-photon polymerization (MPP).[98] A structure of 30 μm × 30 μm × 30 μm was formed using the MPP method, resulting in a PR of −0.13.[98] As per Ali *et al.*[92] a high PR of −0.8 was attained for polymeric auxetic structures that were manufactured through material jetting and dip-in mode on MPP. The direct laser writing (DLW) technique was used to produce micro-structured polymer pentamode metamaterials that have a bulk-to-shear ratio of up to 1000.[99] The use of optical laser lithography to generate flexible laminated heterostructures resulted in better quality pentamode metamaterials,[97] as shown in Fig. 6.

Buckmann *et al.*[100] and Kadic *et al.*[101] utilized a standard MPP system to generate pentamode metamaterials proficient in elastically hiding things. The unfeelability cloak was produced utilizing the MPP setup's dip-in mode. Employing a refractive index matching photoresist, structures may be fabricated that are taller than the objective lens's operating range. The commercial MPP arrangement utilizes Galvo mirror technology to create structures at a high speed of 5 cm $s^{-1}$.[96] One drawback of the MPP system is its restricted construction volume. To address this difficulty, it is considered to divide the design into many sub-designs and fabricate larger structures sequentially. Vat polymerization methods have been used to create mechanical metamaterials with diverse functionality, in addition to extreme materials.

Frenzel *et al.*[102] developed lightweight chiral metamaterials capable of twisting under compression. These metamaterials were created utilizing 3D laser micro printing and demonstrated twists per axial strain surpassing 2°. The self-propagating photopolymer waveguide approach creates open

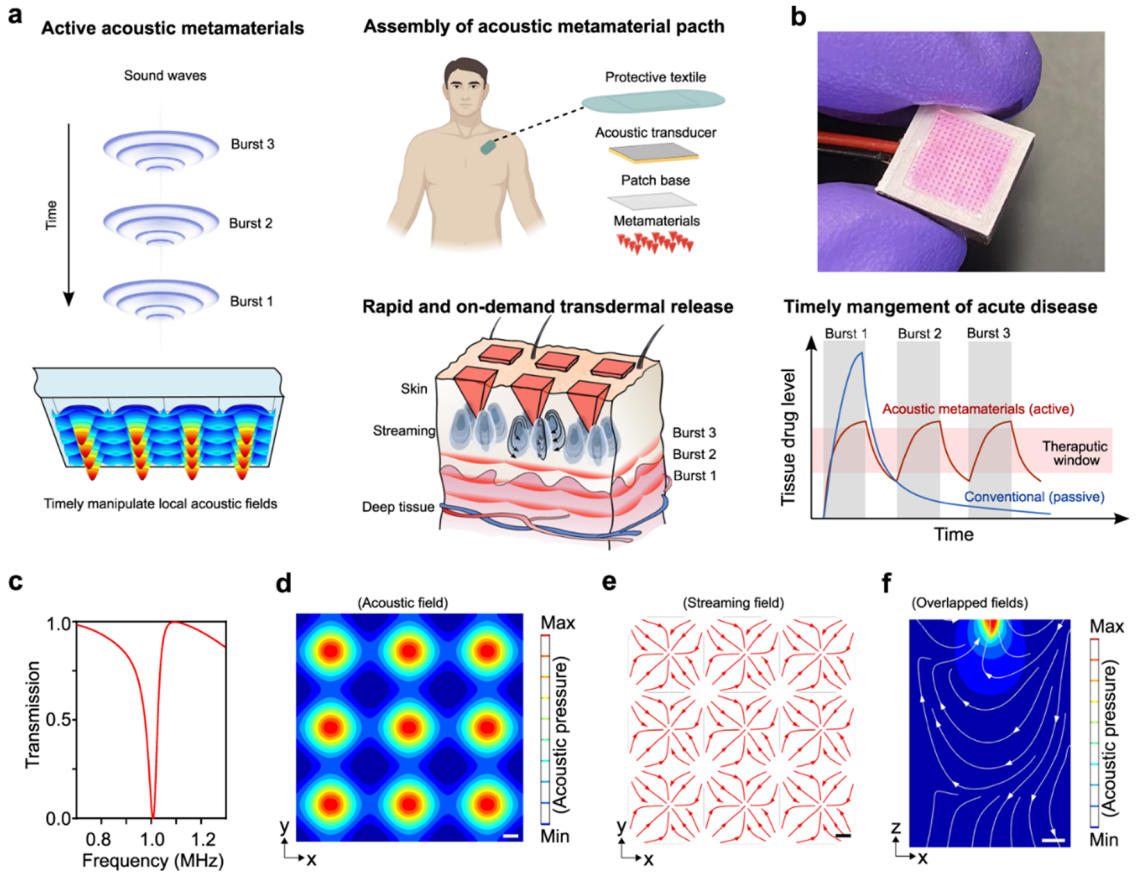


Fig. 5 Transdermal drug delivery that is quick and flexible, powered by active acoustic metamaterials, enabling prompt management of acute illnesses. (a) Diagrams show an active acoustic metamaterial patch delivering drugs quickly and precisely *via* the skin, addressing acute illness and regulating pharmacokinetics in real time. (b) Example of an acoustic metamaterial patch presented. (c) Intended acoustic metamaterials' computed transmission curve. Top view of the metamaterial structures of the simulated acoustic field (d) and acoustic streaming field (e). (f) Side view of one metamaterial structure with overlapping simulated streaming and acoustic fields. This figure was reprinted with permission from Xu *et al.*[83] Copyright 2023 Nature Portfolio.

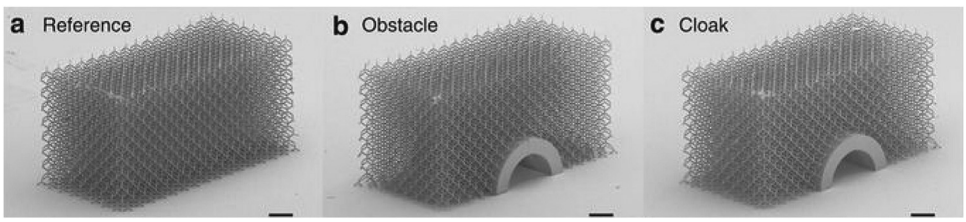


Fig. 6 Unfeelability cloak fabricated to elastically hide the solid cylinder placed underneath the structure.[97] This figure was modified and reprinted with permission from Bückmann *et al.*[97] Copyright 2014 Nature Portfolio.

cellular structures using vat polymerization with collimated ultraviolet (UV) light and a polymer mask. This technology enables large-scale fabrication of micro-lattice structures without compromising the lattice symmetry or diameter. This technology shows promise for creating workable mechanical metamaterials for real-world operations.[103] Polymeric micro-lattices were developed by Jacobsen *et al.*[104] using a photopolymer waveguide technique which was self-propagating. Lightweight hollow-tube nanolattices of high strength and stiffness were developed by Meza *et al.*,[105] these were able to regain their initial shape after compression with over 50% strain. A polymer scaffold was used to 3D print ceramic nanolattices with DLW and using the atomic layer deposition (ALD) method, deposited a thin alumina film, that eliminated the outer walls with concentrated ion beam milling, and etching the internal polymer. Similarly, ceramic (alumina) micro-lattices have been produced utilizing Micro-stereolithography (MSL), ALD, and thermal decomposition.[106]

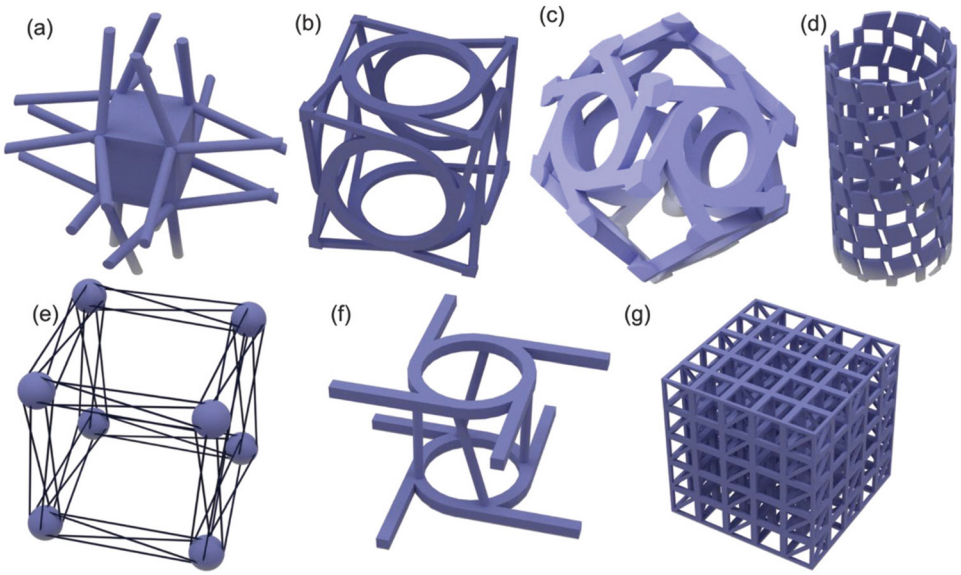


Fig. 7 Motifs of 3D periodic chiral mechanical metamaterials. (a) Unit cell of a cubic-symmetry suggestion; (b) a metamaterial realized and characterized experimentally based on this chiral unit cell; (c) motif as in (b), but with noncubic crystal symmetry; (d) chiral shearing auxetic; (e) conceptual cubic-symmetry model allowing for an approximate analytical treatment based on Euler–Bernoulli beams; (f) uniaxial chiral auxetic; (g) uniaxial lattice composed of an alternation of chiral and achiral units allowing for achieving large characteristic length scales. This figure was modified and reprinted with permission from Carbaton *et al.*[107] Copyright 2019 Wiley Online Library.

This approach has enabled the fabrication of unit cells ranging from 10 to 500 μm. Such lightweight, ultra-stiff lattice structures exhibited the required $(E) \sim \rho$ relationship, independent of material utilized (Fig. 7).

Pyrolyzing polymeric micro-lattices resulted in the creation of glassy carbon micro-lattices. In a study by Eckel *et al.*,[108] self-propagating photopolymer waveguide (SPPW) polymer micro-lattices were converted to ceramic micro-lattices using pyrolysis. Pyrolysis of polymer nanolattices printed using a 3D printer by DLW resulted in glassy carbon nanolattices with theoretical strength and enhanced stiffness-to-density ratio (Fig. 8).[108] In the study of Hedayati *et al.*,[4] the Young's modulus $(E)$ of ultralight micro-lattices was shown to be equivalent to $\bar{\rho}^2$, wherein $\bar{\rho}$ is the ratio of apparent density $(\bar{\rho})$ to base material density $(\bar{\rho}_s)$. Hollow nickel micro-lattices with densities $\bar{\rho} <$ 0.1% demonstrated virtually complete removability for compressive stresses of up to 50%, whereas higher densities exhibited entirely plastic behavior during compression.[109] The mechanical characteristics of the composite micro-lattices were significantly affected by the thickness of NiB layers. Copper micro-lattices of ultra-strength were manufactured using the DLW technique, electroplating, and polymer elimination.[110] Copper micro-lattices exhibit increased stiffness due to size effects resulting from single-crystalline areas in the lattice beams. Two-photon lithography was used to create hollow gold octahedral nanolattices.[111] The polymer nanolattice was subsequently sputtered with columnar gold. The polymer scaffold was eliminated using a concentrated ion beam and oxygen plasma etching. Adjusting the wall layer thickness of Au nanolattices boosted their yield strength by a factor of two. The research found that material size affects strength and stiffness, contrary to the conventional mechanics of cellular solids, which forecast consistent values for all samples.

Multimaterial projection MSL (Fig. 9) was used to create mechanical metamaterials with controllable NTE.[55] To control NTE in a dual-material unit cell it needs to adjust the thermal expansion coefficients and topology of the material. A similar method may be used to achieve a zero-thermal expansion coefficient by balancing positive and negative effects inside the unit cell.[55]

Hybrid vat polymerization procedures are being utilized to create hierarchical hollow tube metamaterials.[96,104,109] Researchers used DLW, ALD, and polymer etching to create hierarchical nanolattices in polymers, and polymer-ceramic composites.[104,109] Titanium nitride hollow tube nanolattices with diameters spanning varying from 10 nm to 100 μm have a tensile yield strength of approximately 1–2 orders of magnitude higher compared to that of bulk material, possibly because of size effects.[112] Apparently, a few drawbacks observed in vat polymerization of metamaterials are limited material selection, as this manufacturing technique mainly supports resins. Residual stress is quite common amongst manufactured parts, leading to reduced accuracy and sensitivity to environmental conditions affects the print quality.[108]

### 4.2 Selective laser melting

The selective laser melting (SLM) technology is widely used to create metallic lattice structures for many purposes, especially automotive[113] and biomedical.[114,115] Ti–6Al–4V ELI, a biomedical-grade titanium alloy, was used to create metamaterials for biomedical purposes.[114] In the study conducted by Wildman *et al.*,[116] the mechanical characteristics of SLM *meta-*

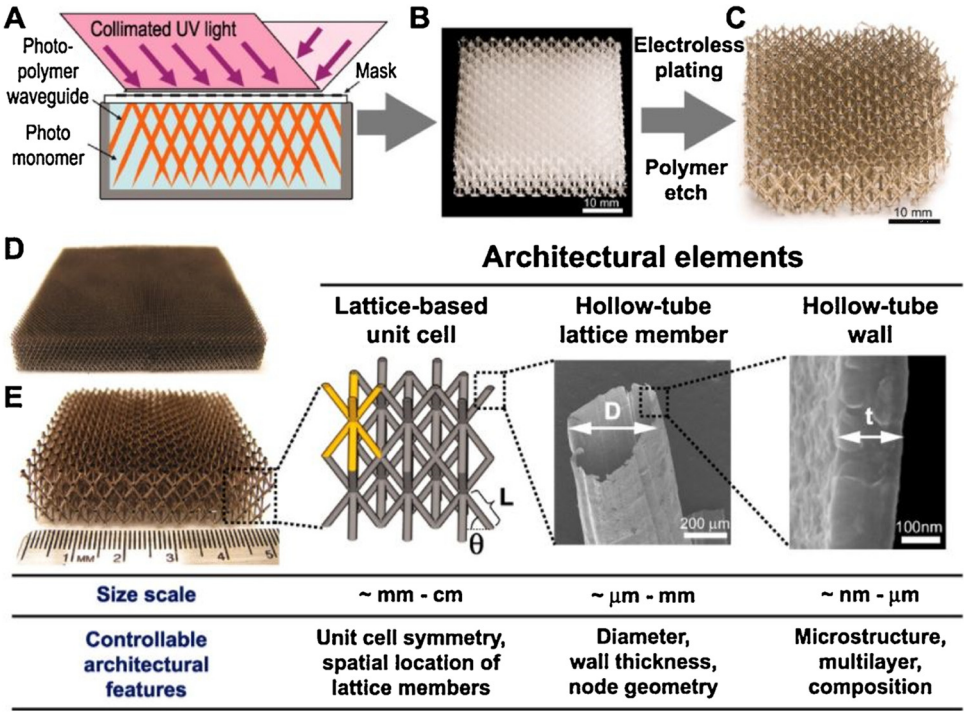


Fig. 8 Structures created utilizing the self-propagation polymer waveguide technology, with feature sizes spanning three orders of magnitude. (A) Basic manufacturing procedure diagram. (B) Polymer template; (C) Ni–P micro-lattice structure created by electroless plating the polymer template and then etching it. (D) and (E) two constructed structures with a breakdown of their building components.[112] This figure was reprinted with permission from Hedayati *et al.*[112] Copyright 2017 the American Institute of Physics.

biomaterials were compared to those of diamond, truncated cuboctahedron, and cubic lattice. SLM has also been used to create auxetic and pentamode structures.[114] Hybrid *meta*-biomaterials were created by combining negative and positive PR's structures to prevent tension-induced failure.[114] SLM was used to create TiNi-based auxetic shape memory alloy structures, which might be used for reusable armor. Titanium alloy (Ti–6Al–4V), a biocompatible and mechanically robust material, was used to create metallic pentamode structures using SLM[115,117] (Fig. 10). The manufactured structures have significantly greater physical features than their polymer equivalents. The pentamode lattices' Young's modulus and strength have been separated from density, resulting in elastic modulus irrespective of permeability. This has important implications for biological uses. Hedayati *et al.*[112] employed vector-based transfer of energy to create pentamode lattice structures having doubled cone connections.[117] In a study of stainless-steel face centred cubic (FCC) metamaterials, hollow lattices demonstrated greater strength and energy absorption over solid lattices of identical density.[106] A common problem observed in SLM is the limited material compatibility and surface roughness of the manufactured part that necessitates post processing for smooth finish.[116]

### 4.3 Selective electron beam melting (SEBM)

SEBM is a powder bed fusion technology that uses electron beams to specifically melt powder beds. This method can create lattice structures having a layer thickness of 50 μm, including auxetic structures made of titanium alloy (Ti–6Al–4V). Various scan methodologies were employed to fabricate unit cells, and the impact of strut size and filling was evaluated. Enhancing the energy utilized to disintegrate the powder from 0.4 to 0.8 J $mm^{-1}$ resulted in thicker connections and changed unit cells. Warmuth *et al.*[118] noticed that the strut dimension considerably impacts the PR and bulk modulus of a structure. The PR remains nearly the same with increasing structural density, but the modulus of elasticity increases. A topology optimization approach called solid isotropic material featuring penalization (SIMP) was applied to create structures having certain mechanical characteristics.[119] SEBM has usually been used to create mathematically optimal structures that are not easily manufactured.[119] Schwerdtfeger *et al.*[119] offered a hybrid method that encompasses optimizing formerly produced structures employing SEBM and including a particular regularization method into the SIMP. The regularization method increases the initial design while reducing the influence on part production. The mix optimization method and Arcam A2 SEBM system were used to achieve a PR of $-0.58 \pm 0.04$. SEBM was used to examine the mechanical traits of lattice structures in several directions. Mechanical testing was implemented on samples having a 4 mm cell size. Finding the behavior of auxetic structures allows scholars to tune them to attain preferred mechanical characteristics.[118]

Elastic metallic structures having mesoscopic components in the region of millimeters were produced *via* volumetric compression of standard metallic foams, which enabled

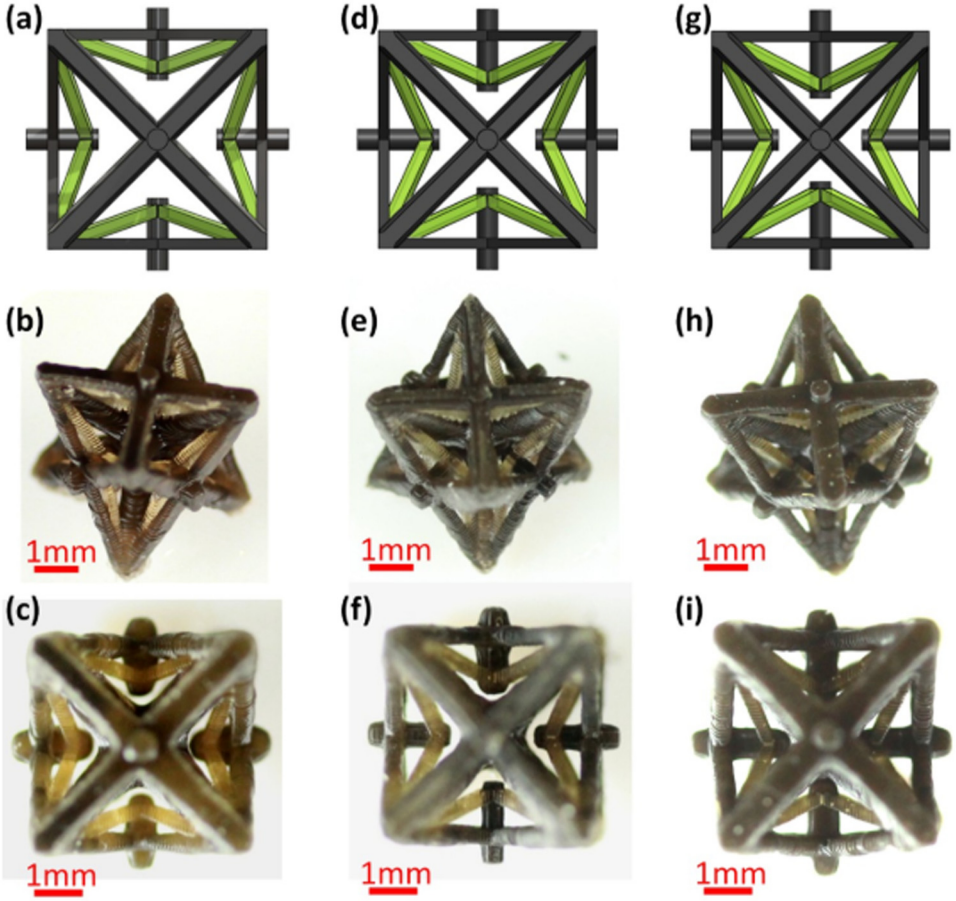


Fig. 9 Metamaterials with tunable negative thermal expansion fabricated using multi-material projection MSL. CAD design (a), (d), and (g), 3D views (b), (e), and (h) and 2D views (c), (f), and (i) of the fabricated unit cell. This figure was modified and reprinted with permission from Wang *et al.*[7] Copyright 2016 American Physical Society.

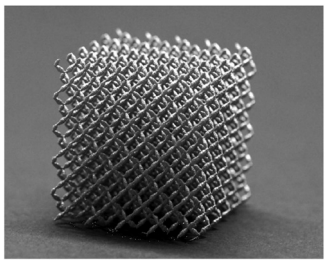

Fig. 10 Pentamode Ti–6Al–4V lattice structure made with SLM.[106] This figure was modified and reprinted with permission from Zadpoor[106] Copyright 2019 ScienceDirect.com by Elsevier.

minimal influence over the resulting structure.[119] Employing AM, a considerable increase in the accuracy of metal cellular structures may be realized.[101] Yang *et al.*[61] developed a computational model for honeycomb auxetic structures and used SEBM to correlate the numerical and experimental findings. The numerical simulation was evaluated by fabricating Ti–6Al–4V lattice structures and accurately measuring the relative density. They also found that when the quantity of unit cells exceeds or equals 3, the features of auxetic honeycomb structures remain unaffected. A primary disadvantage in SEBM is that it subjects the manufactured part to thermal distortion as they undergo rapid heating and cooling cycles.[119]

### 4.4 Material jetting

Three-dimensional auxetic metamaterial structures with prospective applications in energy consumption, and flexible electronics were developed and manufactured *via* inkjet printing. Li *et al.*[120] showed the production of 100 mm × 100 mm structures with a 1 mm beam ligament thickness (Fig. 11). Yang *et al.*[121] created auxetic metamaterials with mechanically modifiable PRs using a multimaterial 3D printer. A large-scale polymer pentamode metamaterial having a bulk to shear modulus ratio of up to 1000 was developed utilizing the polymer ''FullCure850 VeroGray''.[122] While metallic auxetic structures are being actively studied, flexible polymers have received less attention. One illustration is polymeric auxetic re-entrant structure. Employing a conventional Tango Black material for lattice construction resulted in a PR of 1.18.[123] The developed model was contrasted to its 3D CAD design, which revealed that degradation resulting from the potassium

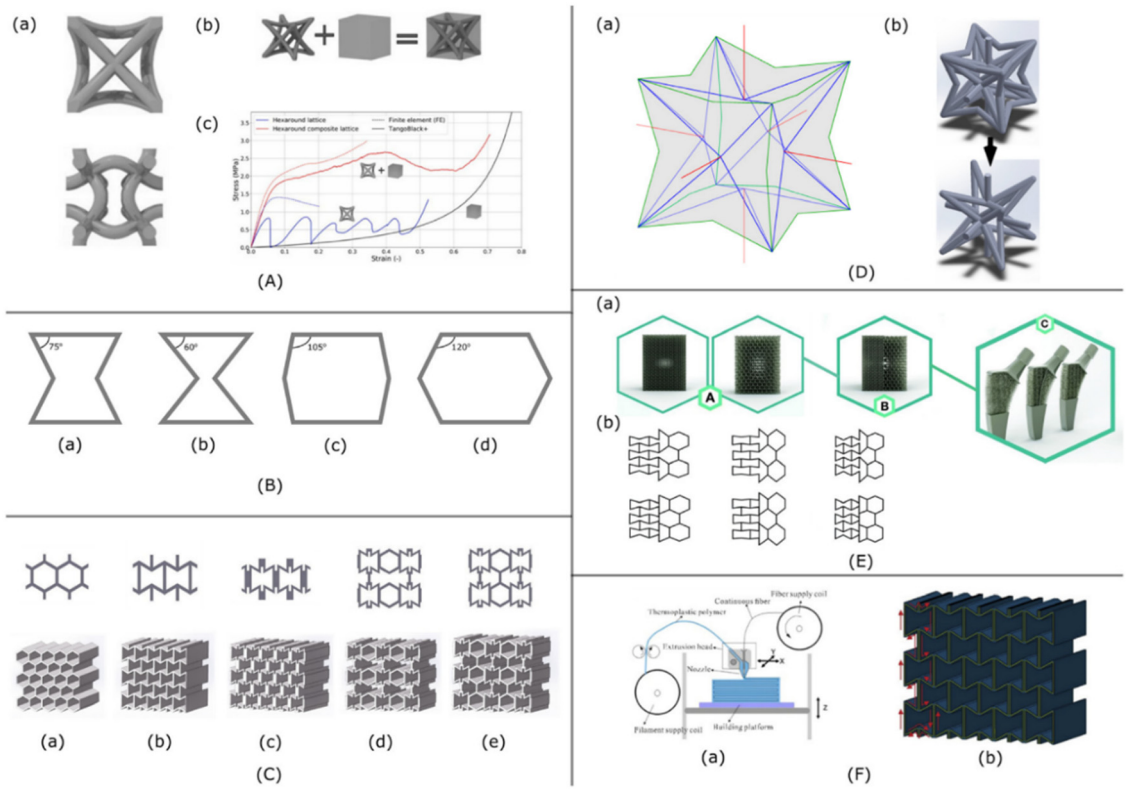


Fig. 11 (A) Auxetic metamaterial structure manufactured using material jetting: (a) hexaround (top) and warmuth (bottom) cells in 2D (b) filling strategy. (c) Stress–strain graph for hexaround lattice, filler, and composite. (B) Schematic design of individual cell dimensions for: (a) −15° re-entrant cells, (b) −30° re-entrant cells, (c) +15° honeycomb cells and (d) +30° honeycomb cells. (C) (a) honeycomb, (b) re-entrant and (c)–(e) hybrid honeycomb structures. (D) (a) An idealized 3D re-entrant unit cell with its struts colored red, blue, and green depending on the strut type, (b) general and lightened re-entrant structure cells. (E) (a) Schematic of (A) auxetic and conventional *meta*-biomaterials, (B) hybrid *meta*-biomaterials and (C) *meta*-implants; and (b) design of six hybrid *meta*-biomaterials. (F) (a) FDM printing setup and (b) schematic of CFRTPC auxetic honeycomb with specific printing path marked in red lines. This figure was modified and reprinted with permission from Mazur and Shishkovsky[124] Copyright 2022 MDPI.

hydroxide cleaning solution and swelling caused by water absorption resulted in regions with high stress and cracking.[123]

Mechanical metamaterials enable soft robots to extend inside pipes using a single actuator. The robot has two soft robotic arms, which impose radial pressure on pipe walls,

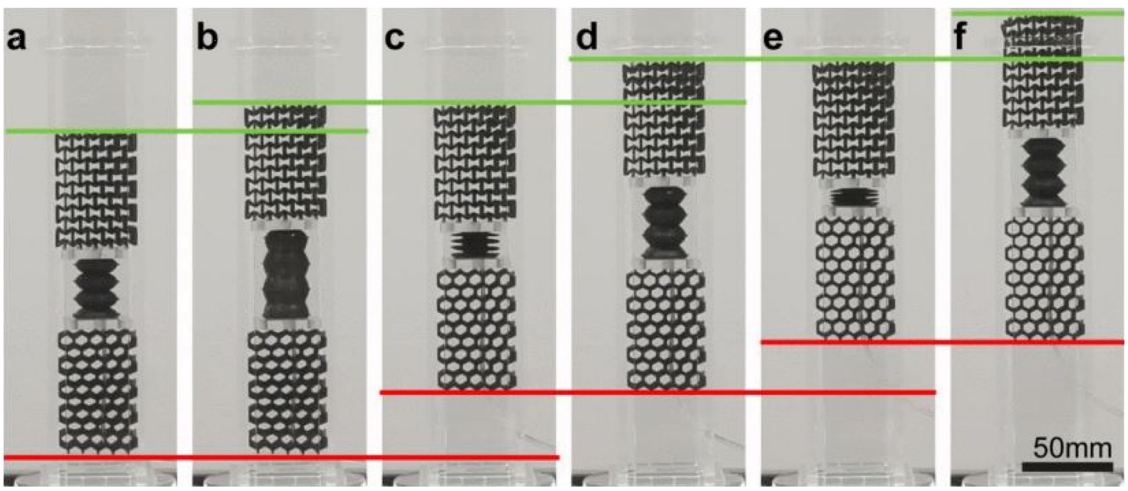


Fig. 12 Single actuator soft robot based on one auxetic metamaterial hand.[128] This figure was reprinted with permission from Mark *et al.*[128] Copyright 2016 IEEE.

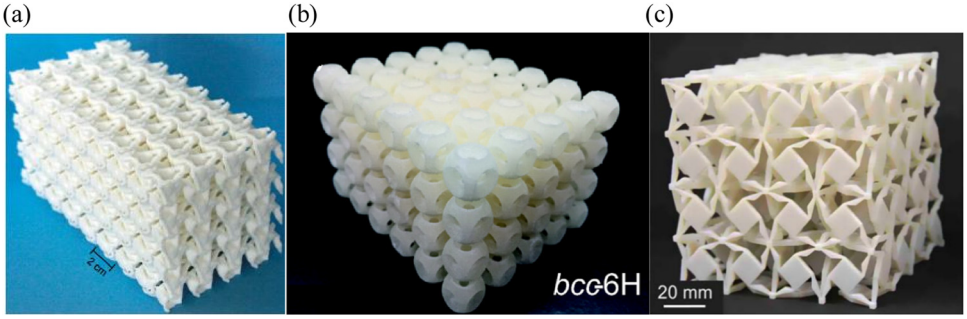


Fig. 13 (a) Polyamide structure manufactured using SLS with a Poisson's ratio of −0.5; (b) soft auxetic lattice structures composed of dual-segment TPU powders;[131] (c) macroscopic polymer auxetic structures have a Poisson's ratio of −0.08.[130] This figure was reprinted with permission from Clausen *et al.*[131] Copyright 2015 Copyright 2019 Wiley Online Library and Ali *et al.*[130] Copyright 2014 Springer Science + Business Media.

differentiated by a linear actuator.[125,126] One arm is composed of auxetic metamaterials, whereas the other is created from an element with a positive PR. When the linear actuator imparts pressure to the arms (Fig. 12), the auxetic structure compresses and reduces radial pressure, allowing the robot to change position. This mechanism is reversed following the contraction stage.[82] Using topology optimization and 3D printing, investigators may customize the PR of produced structures across wide deformation bands. Clausen *et al.*[94] utilized numerical prediction to build 9 structures and printed them with silicon-based elastomeric ink polydimethylsiloxane (PDMS). PRs between −0.8 and 0.8 were attained. The values were somewhat lower than modeling findings; however, this was attributed to tiny changes in the unit cell structure while manufacturing. Inkjet printing is a versatile technology that may create multi-materials structures. Multimaterial auxetic structures exhibit diverse features compared to single material auxetic metamaterials. Wang *et al.*[77] used a Polyjet technique (Connex Objet350 machine) to create dual material auxetic unit cells, demonstrating that these structures are not limited by the balance that exists between PR and Young's modulus. Leveraging flexible connections and solid walls/beams allows for stronger auxetic

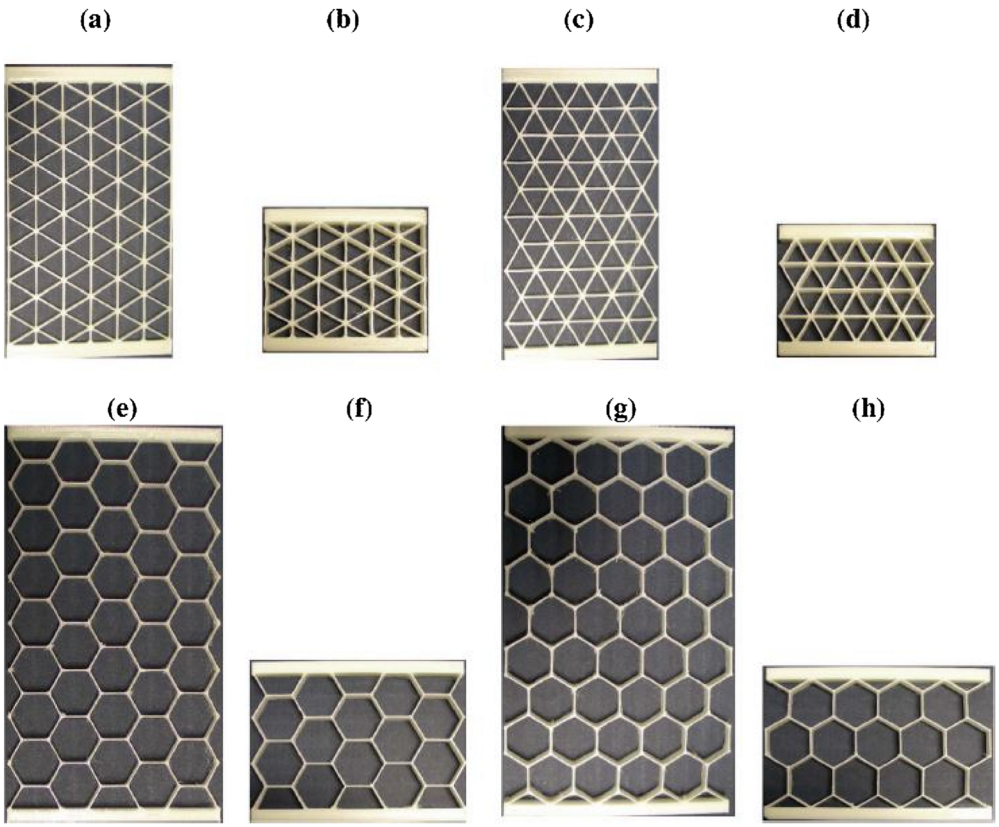


Fig. 14 FDM-printed metamaterial frameworks for testing in mechanical conditions. The frameworks (a), (b), (e), and (f) are used in axial tests and (c), (d), (g), and (h) in transverse directions. The frameworks (a), (c), (e), and (g) were used for tension testing, whereas (b), (d), (f), and (h) were utilized for compression testing.[134] This figure was modified and reprinted with permission from Yuan *et al.*[134] Copyright 2017 ScienceDirect.com by Elsevier.

Table 3 Mechanical properties of different biomedical metamaterials

| Metamaterial | Geometry type | Properties | Deformation mechanism | Ref. |
|---|---|---|---|---|
| Auxetic metamaterial | Honeycomb | (i) Re-entrant hexagonal honeycomb unit cells exhibit high anisotropy and high Young's and shear moduli.<br>(ii) Reducing vertical and diagonal rib thickness can reduce Poisson's ratio and Young's moduli.<br>(iii) 3D structures can be effortlessly designed from the hexagonal honeycomb. | The re-entrant structure's auxetic activity is determined by the cell wall length and angle. When tensile force is exerted, the ribs migrate outward, and the shape expands. | 135 |
| | Chiral | (i) Chiral structures are created by attaching ribs to a center node, which can be a circle, rectangle, or other shape.<br>(ii) Chiral models are on a 2D plane and only show rotational reflections. | Whenever tensile or compressive force is applied uniaxially, the central nodes revolve, causing ligaments to wrap or unravel around them in chiral formations. | 135 and 136 |
| | Arrowhead | (i) The compression starts with the disintegration of triangles, leading to transverse contraction.<br>(ii) The arrowhead structure's stiffness and auxeticity grow with compression strain.<br>(iii) Poisson's ratio may be modified by modifying linkage lengths or rib angles. | The motion of the arrowhead structure is determined by the dimension and angle of the ribs. | 102 |
| Lightweight metamaterial | Honeycomb | (i) Re-entrant hexagonal honeycomb unit cells have considerable anisotropy, which means that their mechanical characteristics depend on the orientation of the force being applied.<br>(ii) Re-entrant hexagonal honeycomb structures have a high Young's modulus, which makes them rigid and resistant to deform during tensile or compressive pressures. | The principal deformation mechanisms in these frameworks involve cell wall bending, as well as compression and extension in various directions. This enables effective energy dissipation. | 102 and 137 |
| | Origami inspired | (i) Origami-inspired structures endure severe deformation without sustaining long-term damage.<br>(ii) Because of their geometrical structure and folding sequences, such materials retain structural stability under a wide range of loads. | When an external stress is enforced, the material folds and unfolds along predefined crease lines, enabling it to store energy and modify shape. | 29 |
| Negative compressibility metamaterials | Porous | (i) Porous negative compressibility metamaterials exhibit negative compressibility when they are subjected to increased pressure.<br>(ii) When subjected to stress, tension, or impact, these metamaterials effectively absorb energy.<br>(iii) The size, shape and distribution of pores could be varied by changing the stiffness and compressibility of these metamaterials. | When pressure is introduced to the metamaterial, the pores enlarge instead of compressing. This enlargement might result from the motion of the material around the pores or the rearranging of the pores themselves. | 37 and 45 |
| | Spring like | (i) The capacity of spring-like negative compressibility metamaterials to expand in response to pressure increases is their most distinguishing feature.<br>(ii) Spring-like negative compressibility metamaterials may go through reversible deformation cycles, expanding and contracting when pressure is imposed and released. | When you apply pressure to the metamaterial, the spring-like parts start to uncoil. This uncoiling action permits the material to enlarge in volume instead of compressing. The deformation process is frequently nonlinear since spring-like materials may originally oppose displacement before abruptly uncoiling and expanding. | 45 |
| Pentamode metamaterials | Lattice structures | (i) A lattice structure pentamode metamaterials have a very high bulk modulus, making them particularly resistant to compressive deformation.<br>(ii) These metamaterials have a low shear modulus, which allows them to quickly transform under shear force. The lattice structure is designed to have low shear stiffness whilst preserving compressive strength, resulting in a fluid-like reaction to shear forces.<br>(iii) These metamaterials possess anisotropic mechanical characteristics and are mainly regulated by changes in the design and orientation of the lattice members. | A lattice structure, Pentamode metamaterials possess a modest shear modulus, causing them to be easily deformed by shear force. Under shear force, the lattice components can buckle or shift, according to the structure's architecture and shape. | 55 and 56 |
| | Metafluids | (i) Metafluid pentamode metamaterials have very high bulk modulus but very low shear modulus. They readily deform when subjected to shear stresses, displaying fluid-like characteristics like flow, and bending while maintaining solid structures.<br>(ii) Due to these properties, these types of metamaterials exhibit excellent acoustic properties. | When a compressive load is exerted, the material conveniently bears the force while avoiding volume change. Given their extremely low shear modulus, these metamaterials behave similarly to fluids under shear stress. They can be easily deformed, twisted, and flow in response to shear loads. Under shear force, Metafluid pentamode metamaterials may buckle or reorient their microstructure. This procedure enables the material to withstand shear deformation while maintaining overall coherence and rigidity. | 55 |

constructions. Buckling in the middle of the walls reduces auxeticity. However, in the 2D material auxetic structure, flexible joints maintain a stable negative PR during high deformations.[127]

### 4.5 Selective laser sintering (SLS)

SLS had been employed in the production of macroscopic auxetic materials. Andreassen *et al.*[103] used topology optimization to develop 3D materials with periodic structures, achieving a Poisson's ratio of −0.5 and a bulk modulus of 0.2% for homogeneous base materials (Fig. 13a). This research presents individual material structures made from polyamide utilizing SLS machinery.[103] Wang *et al.*[129] employed SLS technology to produce 3D soft auxetic lattice networks with dual-segment thermoplastic polyurethane (TPU) powders that operate in hard and soft states (Fig. 13b). The auxetic cells have 3D body-centered cubic (BCC) and simple cubic (SC) structures made of elastomeric 6- or 12-hole spherical shells. Li *et al.*[130] used SLS to create large-scale polymer auxetic structures with a Poisson's ratio of −0.8 (Fig. 13c). With is technique, high energy consumption is common due to prolonged laser use and high-temperature requirements.[131]

### 4.6 Fused deposition modeling (FDM)

FDM was used to deposit soft polylactide (PLA) material, resulting in rhombohedral and hexagonal unit cells. The designs were built using a printing speed of 40 mm $s^{-1}$ and a layer thickness of 0.2 mm.[130] The beam-like components were 1 mm thick and 16 mm long. The mechanical traits of such structures were explored under tension and compression in the substantial deformation domain (Fig. 14). It was noticed that metamaterials have different behaviors in both axial and transverse directions. This raises anisotropy issues on the metamaterials due to layer wise depositions, reducing the effectiveness and uniformity of the metamaterial producing parts that have rough surfaces and visible layer lines. These parts further require post-processing that increases the time and costs.[132] Additionally, the metamaterial reaction changes with compression and tension. These findings exhibit how the form, kind, and size of the unit cell have a major impact on the metamaterial reaction.[130] Using FDM, biomedical metamaterial devices like tailored bone implants and prostheses with tailored porosity and mechanical qualities that closely mirror those of natural bone, by including various cell types, especially shear cells into the design.[133] Research was conducted on the failure mechanism, absorption of energy, and multi-hit potential of polymer FDM manufactured *meta*-sandwich structures composed of isomax, octet, cubic, and auxetic cells.[132]

## 5 Potential trends, challenges and solutions

Overall, this review reiterates to the fact that metamaterials have been widely used in the field of biomedical engineering in comparison to any other field. However, it is important to note that metamaterials may pose a certain set of challenges based on their properties and structural complexity. This section summarizes the potential future applications of the metamaterials, the challenges that may occur and ways to overcome these challenges (Table 3).

- Biomedical metamaterials tend to heavily rely on AI and machine learning for specific applications that require fine tuning. These tools could not only predict the mechanical properties such as stiffness, strength, *etc.*, but also optimize them. This way, development of personal medical devices and implants is hugely possible.
- The current AM techniques implemented for the manufacture of biomedical metamaterials enable intricate and complex designs. However, scaling up production with high resolution and repeatability has been quite challenging. Future trends point out the incorporation of more robust and multi-functional 3D printers that could produce batches of biomaterials that have consistent mechanical properties and minimal deficiencies.
- Biomaterials are more embedded into healthcare and as a result, it is important that they remain compatible and avoid any kind of adverse reactions with the bodily fluids. There has been an increasing demand to include biomaterials that are more environmentally friendly with their manufacturing processes addressing sustainable concerns, while keeping their performance at top priority in biomedical applications.
- Metamaterials could be optimized through lightweight and optimized designs by using reduced material and energy consumption during manufacturing processes. This could potentially be overcome through advanced 3D printing techniques such as multi-material 3D printing and fused deposit modelling (FDM), which focus on minimizing waste material generation during fabrication. These types of innovations will ensure sustainability of the metamaterial without compromising on the mechanical properties of the metamaterials.
- Biomedical applications must withstand varying mechanical loads with longer periods. Future research must focus on optimizing properties such as elasticity, stiffness and toughness, ensuring that these perform reliably in critical applications such as load bearing implants and scaffolds.
- The present production costs that are used for metamaterials are high with limited accessibility. The implementation of more cost-effective manufacturing techniques that can optimize material usage is crucial, so that these materials could be adapted in the biomedical field, making improved treatments with affordability.

## Data availability

Data are available upon request to the corresponding author.

## Conflicts of interest

There are no conflicts to declare.

## Acknowledgements

This research was supported by the Structures and Materials (S&M) Research Lab of Prince Sultan University. Furthermore, the authors acknowledge the support of Prince Sultan University for paying the article processing charges (APC) of this publication.

## References

1 S. Ahmadi, R. Hedayati, Y. Li, K. Lietaert, N. Tümer, A. Fatemi, C. Rans, B. Pouran, H. Weinans and A. Zadpoor, Fatigue performance of additively manufactured meta-biomaterials: the effects of topology and material type, *Acta Biomater.*, 2018, **65**, 292–304.

2 Z. Jia, F. Liu, X. Jiang and L. Wang, Engineering lattice metamaterials for extreme property, programmability, and multifunctionality, *J. Appl. Phys.*, 2020, **127**, 150901, DOI: 10.1063/5.0004724.

3 Y. Wang, L. Zhang, S. Daynes, H. Zhang, S. Feih and M. Y. Wang, Design of graded lattice structure with optimized mesostructures for additive manufacturing, *Mater. Des.*, 2018, **142**, 114–123.

4 R. Hedayati, S. Ahmadi, K. Lietaert, B. Pouran, Y. Li, H. Weinans, C. Rans and A. Zadpoor, Isolated and modulated effects of topology and material type on the mechanical properties of additively manufactured porous biomaterials, *J. Mech. Behav. Biomed. Mater.*, 2018, **79**, 254–263.

5 A. Rahimizadeh, Z. Nourmohammadi, S. Arabnejad, M. Tanzer and D. Pasini, Porous architected biomaterial for a tibial-knee implant with minimum bone resorption and bone-implant interface micromotion, *J. Mech. Behav. Biomed. Mater.*, 2018, **78**, 465–479.

6 J. Wu, N. Aage, R. Westermann and O. Sigmund, Infill optimization for additive manufacturing—approaching bone-like porous structures, *IEEE Trans. Visual Comput. Graphics*, 2018, **24**(2), 1127–1140.

7 X. Wang, S. Xu, S. Zhou, W. Xu, M. Leary, P. Choong, M. Qian, M. Brandt and Y. M. Xie, Topological design, and additive manufacturing of porous metals for bone scaffolds and orthopaedic implants: a review, *Biomaterials*, 2016, **83**, 127–141.

8 C. Yan, L. Hao, A. Hussein and P. Young, Ti–6Al–4V triply periodic minimal surface structures for bone implants fabricated via selective laser melting, *J. Mech. Behav. Biomed. Mater.*, 2015, **51**, 61–73.

9 B. Van Hooreweder, K. Lietaert, B. Neirinck, N. Lippiatt and M. Wevers, CoCr F75 scaffolds produced by additive manufacturing: influence of chemical etching on powder removal and mechanical performance, *J. Mech. Behav. Biomed. Mater.*, 2017, **70**, 60–67.

10 H. Montazerian, E. Davoodi, M. Asadi-Eydivand, J. Kadkhodapour and M. Solati-Hashjin, Porous scaffold internal architecture design based on minimal surfaces: a compromise between permeability and elastic properties, *Mater. Des.*, 2017, **126**, 98–114.

11 Q. Wang, J. A. Jackson, Q. Ge, J. B. Hopkins, C. M. Spadaccini and N. X. Fang, Lightweight mechanical metamaterials with tunable negative thermal expansion, *Phys. Rev. Lett.*, 2016, **117**(17), 175901.

12 M. K. Ravari, S. N. Esfahani, M. T. Andani, M. Kadkhodaei, A. Ghaei, H. Karaca and M. Elahinia, On the effects of geometry, defects, and material asymmetry on the mechanical response of shape memory alloy cellular lattice structures, *Smart Mater. Struct.*, 2016, **25**(2), 025008.

13 Z. G. Nicolaou and A. E. Motter, Mechanical metamaterials with negative compressibility transitions, *Nat. Mater.*, 2012, **11**(7), 608.

14 L. Liu, P. Kamm, F. García-Moreno, J. Banhart and D. Pasini, Elastic and failure response of imperfect three-dimensional metallic lattices: the role of geometric defects induced by Selective Laser Melting, *J. Mech. Phys. Solids*, 2017, **107**, 160–184.

15 Y. Tang and J. Yin, Design of cut unit geometry in hierarchical kirigami-based auxetic metamaterials for high stretchability and compressibility, *Extreme Mech. Lett.*, 2017, **12**, 77–85.

16 K. Wang, Y.-H. Chang, Y. Chen, C. Zhang and B. Wang, Designable dual-material auxetic metamaterials using three-dimensional printing, *Mater. Des.*, 2015, **67**, 159–164.

17 A. A. Zadpoor, Design for additive bio-manufacturing: from patient-specific medical devices to rationally designed meta-biomaterials, *Int. J. Mol. Sci.*, 2017, **18**(8), 1607.

18 C.-X. Lu, M.-T. Hsieh, Z.-F. Huang, C. Zhang, Y. Lin and Q. Shen, *et al.*, Architectural design and additive manufacturing of mechanical metamaterials: A review, *Engineering*, 2022, **17**, 44–63, DOI: 10.1016/j.eng.2021.12.023.

19 D. Mousanezhad, B. Haghpanah, R. Ghosh, A. M. Hamouda, H. Nayeb-Hashemi and A. Vaziri, Elastic properties of chiral, anti-chiral, and hierarchical honeycombs: A simple energy-based approach, *Theor. Appl. Mech. Lett.*, 2016, **6**(2), 81–96, DOI: 10.1016/j.taml.2016.02.004.

20 C. Lv, D. Krishnaraju, G. Konjevod, H. Yu and H. Jiang, Origami based mechanical metamaterials, *Sci. Rep.*, 2014, **4**(1), 5979, DOI: 10.1038/srep05979.

21 Y. Yang and Z. You, A Modular Origami-inspired Mechanical Metamaterial, *arXiv*, 2020, preprint, DOI: 10.48550/arXiv.2012.09567.

22 C.-X. Lu, M.-T. Hsieh, Z.-F. Huang, C. Zhang, Y. Lin and Q. Shen, *et al.*, Architectural design and additive manufacturing of mechanical metamaterials: A review, *Engineering*, 2022, **17**, 44–63, DOI: 10.1016/j.eng.2021.12.023.

23 X. Zhang, Y.-J. Wang, B. Ding and X. Li, Design, fabrication, and mechanics of 3D micro-/Nanolattices, *Small*, 2020, **16**(15), 1902842, DOI: 10.1002/smll.201902842.

24 J.-J. Do Rosário, J.-B. Berger, E.-T. Lilleodden, R. M. McMeeking and G. A. Schneider, The stiffness and strength of metamaterials based on the inverse opal architecture, *Extreme Mech. Lett.*, 2017, **12**, 86–96, DOI: 10.1016/j.eml.2016.07.006.

25 J.-J. Do Rosário, E.-T. Lilleodden, M. Waleczek, R. Kubrin, A. Y. Petrov and P. N. Dyachenko, *et al.*, Self-assembled

ultra-high strength, ultra stiff mechanical metamaterials based on inverse opals, *Adv. Eng. Mater.*, 2015, **17**(10), 1420–1424, DOI: 10.1002/adem.201500118.

26 Z.-M. Jiang and J.-H. Pikul, Centimeter-scale crack-free self-assembly for ultra-high tensile strength metallic nanolattices, *Nat. Mater.*, 2021, **20**(11), 1512–1518, DOI: 10.1038/s41563-021-01039-7.

27 D. Prall and R.-S. Lakes, Properties of a chiral honeycomb with a Poisson's ratio of -1, *Int. J. Mech. Sci.*, 1997, **39**(3), 305–314, DOI: 10.1016/s0020-7403(96)00025-2.

28 K.-W. Wojciechowski, Two-dimensional isotropic system with a negative Poisson ratio, *Phys. Lett. A*, 1989, **137**(1), 60–64, DOI: 10.1016/0375-9601(89)90971-7.

29 T. Tomohiro, Designing freeform origami tessellations by generalizing Resch's patterns, *J. Mech. Des.*, 2013, **135**(11), 180, DOI: 10.1115/1.4025389.

30 H.-S. Han, V. Sorokin, L.-H. Tang and D. Cao, Origami-based tunable mechanical memory metamaterial for vibration attenuation, *Mech. Syst. Signal Process.*, 2023, **188**, 110033, DOI: 10.1016/j.ymssp.2022.110033.

31 M. Schenk and S.-D. Guest, Geometry of Miura-folded metamaterials, *Proc. Natl. Acad. Sci. U. S. A.*, 2013, **110**(9), 3276–3281, DOI: 10.1073/pnas.1217998110.

32 K.-C. Cheung, T. Tachi, S. Calisch and K. Miura, Origami interleaved tube cellular materials, *Smart Mater. Struct.*, 2014, **23**(9), 094012–94110, DOI: 10.1088/0964-1726/23/9/094012.

33 R. Gatt, M. V. Wood, A. Gatt, F. Zarb, C. Formosa, K. M. Azzopardi, A. Casha, T. P. Agius, P. Schembri-Wismayer and L. Attard, Negative Poisson's ratios in tendons: an unexpected mechanical response, *Acta Biomater.*, 2015, **24**, 201–208.

34 H. M. A. Kolken and A. A. Zadpoor, Auxetic mechanical metamaterials, *RSC Adv.*, 2017, **7**, 5111–5129, DOI: 10.1039/c6ra27333e.

35 A. Alderson, K.-L. Alderson, G. Chirima, N. Ravirala and K. Zied, The inplane linear elastic constants and out-of-plane bending of 3-coordinated ligament and cylinder-ligament honeycombs, *Compos. Sci. Technol.*, 2010, **70**(7), 1034–1041, DOI: 10.1016/j.compscitech.2009.07.010.

36 J.-T.-B. Overvelde and K. Bertoldi, Relating pore shape to the non-linear response of periodic elastomeric structures, *J. Mech. Phys. Solids*, 2014, **64**, 351–366, DOI: 10.1016/j.jmps.2013.11.014.

37 H. Wang, Y. Lyu, S. Bosiakov, H. Zhu and Y. Ren, A review on the mechanical metamaterials and their applications in the field of biomedical engineering, *Front. Mater.*, 2023, **10**, 1273961, DOI: 10.3389/fmats.2023.1273961.

38 K. Bertoldi, M.-C. Boyce, S. Deschanel, S. Prange and T. Mullin, Mechanics of deformation-triggered pattern transformations and super elastic behavior in periodic elastomeric structures, *J. Mech. Phys. Solids*, 2008, **56**(8), 2642–2668, DOI: 10.1016/j.jmps.2008.03.006.

39 B. Florijn, C. Coulais and M. Hecke, Programmable mechanical metamaterials, *Phys. Rev. Lett.*, 2014, **113**(17), 175503, DOI: 10.1103/physrevlett.113.175503.

40 J. Chung and A.-M. Waas, Compressive response of circular cell polycarbonate honeycombs under inplane biaxial static and dynamic loading. Part I: experiments, *Int. J. Impact Eng.*, 2002, **27**(7), 729–754, DOI: 10.1016/s0734-743x(02)00011-8.

41 D. Yang, L.-H. Jin, R.-V. Martinez, K. Bertoldi, G. M. Whitesides and Z. Suo, Phase-transforming and switchable metamaterials, *Extreme Mech. Lett.*, 2016, **6**, 1–9, DOI: 10.1016/j.eml.2015.11.004.

42 X.-Q. Cao, J.-Y. Guo, Y.-Q. Li, Q. Zhang, Z. Zhou and J. Sun, *et al.*, Prediction of post buckling characteristics of perforated metamaterial cylindrical shells under axial compression, *Acta Mech. Solida Sin.*, 2023, **36**(3), 428–442, DOI: 10.1007/s10338-023-00378-z.

43 X.-J. Tan, S. Chen, B. Wang, J. Tang, L. Wang and S. Zhu, *et al.*, Real-time tunable negative stiffness mechanical metamaterial, *Extreme Mech. Lett.*, 2020, **41**, 100990, DOI: 10.1016/j.eml.2020.100990.

44 R.-H. Baughman, S. Stafström, C.-X. Cui and S. O. Dantas, Materials with negative compressibilities in one or more dimensions, *Sci. Am. Assoc. Adv. Sci.*, 1998, **279**(5356), 1522–1524, DOI: 10.1126/science.279.5356.1522.

45 Y.-M. Xie, X.-Y. Yang, J.-H. Shen, X. Yan, A. Ghaedizadeh and J. Rong, *et al.*, Designing orthotropic materials for negative or zero compressibility, *Int. J. Solids Struct.*, 2014, **51**(23), 4038–4051, DOI: 10.1016/j.ijsolstr.2014.07.024.

46 Z.-G. Nicolaou and A.-E. Motter, Longitudinal inverted compressibility in super-strained metamaterials, *J. Stat. Phys.*, 2013, **151**(6), 1162–1174, DOI: 10.1007/s10955-013-0742-8.

47 A.-B. Cairns and A.-L. Goodwin, Negative linear compressibility, *Phys. Chem. Chem. Phys.*, 2015, **204**(17), 20449–20465, DOI: 10.1039/c5cp00442j.

48 W. Li, M.-R. Probert, M. Kosa, T. D. Bennett, A. Thirumurugan and R. P. Burwood, *et al.*, Negative linear compressibility of a metal-organic framework, *J. Am. Chem. Soc.*, 2012, **134**(29), 11940–11943, DOI: 10.1021/ja305196u.

49 A. Ghaedizadeh, J.-H. Shen, X. Ren and Y. M. Xie, Designing composites with negative linear compressibility, *Mater. Des.*, 2017, **131**, 343–357, DOI: 10.1016/j.matdes.2017.06.026.

50 W.-Z. Cai, A. Gładysiak, M. Anioła, V. J. Smith, L. J. Barbour and A. Katrusiak, Giant negative area compressibility tunable in a soft, porous framework material, *J. Am. Chem. Soc.*, 2015, **137**(29), 9296–9301, DOI: 10.1021/jacs.5b03280.

51 S.-A. Hodgson, J. Adamson, S.-J. Hunt, M. J. Cliffe, A. B. Cairns and A. L. Thompson, *et al.*, Negative area compressibility in silver(I) tricyanomethanide, *Chem. Commun. Camb. Engl.*, 2014, **50**(40), 5264–5266, DOI: 10.1039/c3cc47032f.

52 I.-E. Collings, M.-G. Tucker, D.-A. Keen and A. L. Goodwin, Geometric switching of linear to area negative thermal expansion in uniaxial metal-organic frameworks, *CrystEngComm*, 2014, **16**(17), 3498–3506, DOI: 10.1039/c3ce42165a.

53 M. Tortora, P. Zajdel, A.-R. Lowe, M. Chorążewski, J. B. Leão and G. V. Jensen, *et al.*, Giant negative compressibility by liquid intrusion into superhydrophobic flexible nanoporous frameworks, *Nano Lett.*, 2021, **21**(7), 2848–2853, DOI: 10.1021/acs.nanolett.0c04941.

54 M. Kim, K. Lee, E. Bok, D. Hong, J. Seo and S. H. Lee, Broadband muffler by merging negative density and negative compressibility, *Appl. Acoust.*, 2023, **208**, 109373, DOI: 10.1016/j.apacoust.2023.109373.
55 J. Christensen, M. Kadic, M. Wegener and O. Kraft, Vibrant times for mechanical metamaterials, *MRS Commun.*, 2015, **5**, 453–462, DOI: 10.1557/mrc.2015.51.
56 M. Kadic, T. Bückmann, R. Schittny and M. Wegener, On anisotropic versions of three-dimensional pentamode metamaterials, *New J. Phys.*, 2013, **15**(2), 023029, DOI: 10.1088/1367-2630/15/2/023029.
57 G.-W. Milton and A.-V. Cherkaev, Which elasticity tensors are realizable?, *J. Eng. Mater. Technol.*, 1995, **117**(4), 483–493, DOI: 10.1115/1.2804743.
58 O. Sigmund, Tailoring materials with prescribed elastic properties, *Mech. Mater.*, 1995, **20**(4), 351–368, DOI: 10.1016/0167-6636(94)00069-7.
59 A. Martin, M. Kadic, R. Schittny, T. Bückmann and M. Wegener, Phonon band structures of three-dimensional pentamode metamaterials, *Phys. Rev. B: Condens. Matter.*, 2012, **86**(15), 155116–164181, DOI: 10.1103/physrevb.86.155116.
60 T.-B. Liang, M. He, H.-W. Dong, L. Xia and X. Huang, Ultrathin waterborne acoustic metasurface for uniform diffuse reflections, *Mech. Syst. Signal Process.*, 2023, **192**, 110226, DOI: 10.1016/j.ymssp.2023.110226.
61 L. Yang, O. Harrysson, H. West and D. Cormier, Mechanical properties of 3D reentrant honeycomb auxetic structures realized via additive manufacturing, *Int. J. Solids Struct.*, 2015, **69–70**, 475–490, DOI: 10.1016/j.ijsolstr.2015.05.005.
62 J.-N. Grima, P.-S. Farrugia, R. Gatt and D. Attard, On the auxetic properties of rotating rhombi and parallelograms: A preliminary investigation, *Phys. Status Solidi B*, 2008, **245**(3), 521–529, DOI: 10.1002/pssb.200777705.
63 Z. Guo, W. Liu, N. Li and G. Li, Bioinspired hierarchical honeycomb structures: Experiments and modeling, *J. Mech. Phys. Solids*, 2016, **96**, 561–577.
64 N. Hüsing and U. Schubert, Aerogels airy materials: Chemistry, structure, and properties, *Angew. Chem., Int. Ed.*, 1998, **37**(1–2), 22–45.
65 J.-N. Grima and K.-E. Evans, Auxetic behavior from rotating squares, *J. Mater. Sci. Lett.*, 2000, **19**(17), 1563–1565, DOI: 10.1023/a:1006781224002.
66 J.-N. Grima and K.-E. Evans, Auxetic behavior from rotating triangles, *J. Mater. Sci.*, 2006, **41**(10), 3193–3196, DOI: 10.1007/s10853-006-6339-8.
67 J.-N. Grima, A. Alderson and K.-E. Evans, Negative Poisson's ratios from rotating rectangles, *Comput. Methods Sci. Technol.*, 2004, **10**(2), 137–145, DOI: 10.12921/cmst.2004.10.02.137-145.
68 J.-N. Grima, R. Gatt, A. Alderson and K. E. Evans, On the auxetic properties of Rotating rectangles with different connectivity, *J. Phys. Soc. Jpn.*, 2005, **74**(10), 2866–2867, DOI: 10.1143/jpsj.74.2866.
69 J.-N. Grima, R. Gatt and P.-S. Farrugia, On the properties of auxetic metatetrachiral structures, *Phys. Status Solidi B*, 2008, **245**(3), 511–520, DOI: 10.1002/pssb.200777704.
70 J.-N. Grima and R. Gatt, Perforated sheets exhibiting negative Poisson's ratios, *Adv. Eng. Mater.*, 2010, **12**(6), 460–464, DOI: 10.1002/adem.201000005.
71 L. Mizzi, D. Attard, K.-E. Evans, R. Gatt and J. N. Grima, Auxetic mechanical metamaterials with diamond and elliptically shaped perforations, *Acta Mech.*, 2021, **232**(2), 779–791, DOI: 10.1007/s00707-020-02881-7.
72 X. Huang and S. Blackburn, Developing a new processing route to manufacture honeycomb ceramics with negative Poisson's ratio, *Key Eng. Mater.*, 2002, **206**, 201–204.
73 K. L. Alderson, R. S. Webber and K. E. Evans, Microstructural evolution in the processing of auxetic microporous polymers, *Phys. Status Solidi*, 2007, **244**, 828–841.
74 K. E. Evans and B. D. Caddock, Microporous materials with negative Poisson's ratios. II. Mechanisms and interpretation, *J. Phys. D: Appl. Phys.*, 1989, **22**, 1883–1887.
75 K. E. Evans, J. P. Donoghue and K. L. Alderson, The Design, Matching and Manufacture of Auxetic Carbon Fibre Laminates, *J. Compos. Mater.*, 2004, **38**, 95–106.
76 K. E. Evans and K. L. Alderson, The static and dynamic moduli of auxetic microporous polyethylene, *J. Mater. Sci. Lett.*, 1992, **11**, 1721–1724.
77 H. Wang, S.-H. Xiao and C. Zhang, Novel planar auxetic metamaterial perforated with orthogonally aligned oval-shaped holes and machine learning solutions, *Adv. Eng. Mater.*, 2021, **23**(7), 2100102, DOI: 10.1002/adem.202100102.
78 B.-D. Caddock and K.-E. Evans, Microporous materials with negative Poisson's ratios. II. Mechanisms and interpretation, *J. Phys. D: Appl. Phys.*, 1989, **22**(12), 1883–1887, DOI: 10.1088/0022-3727/22/12/013.
79 B.-D. Caddock and K.-E. Evans, Microporous materials with negative Poisson's ratios. I. Microstructure and mechanical properties, *J. Phys. D: Appl. Phys.*, 1989, **22**(12), 1877–1882, DOI: 10.1088/0022-3727/22/12/012.
80 M. Schenk and S.-D. Guest, Geometry of miura-folded metamaterials, *Proc. Natl. Acad. Sci. U. S. A.*, 2013, **110**(9), 3276–3281, DOI: 10.1073/pnas.1217998110.
81 R. Lakes, Advances in negative Poisson's ratio materials, *Adv. Mater. Sci. Eng.*, 1996, **5**(4), 293–296, DOI: 10.1155/S1359646196000200.
82 N. Hüsing and U. Schubert, Aerogels airy materials: Chemistry, structure, and properties, *Angew. Chem., Int. Ed.*, 1998, **37**(1–2), 22–45.
83 J. Xu, H. Cai, Z. Wu, X. Li, C. Tian, Z. Ao, V. C. Niu, X. Xiao, L. Jiang, M. Khodoun, M. Rothenberg, K. Mackie, J. Chen, L. P. Lee and F. Guo, Acoustic metamaterials-driven transdermal drug delivery for rapid and on-demand management of acute disease, *Nat. Commun.*, 2023, **14**(1), 869, DOI: 10.1038/s41467-023-36581-2.
84 H. Mehboob, *Biomechanical Performance Evaluation of Composite Metamaterial Implant with 3d Printing Approach for Lumbar Interbody Fusion Surgery: A Finite Element Study*, Elsevier, 2022, DOI: 10.1016/j.compstruct.2022.116379.
85 A. Ouldyerou, L. Aminallaha, A. Merdji, A. Mehboob and H. Mehboob, *Finite element analyses of porous dental*

*implant designs based on 3D printing concept to evaluate biomechanical behaviors of healthy and osteoporotic bones*, Taylor & Francis, 2022, DOI: 10.1080/15376494.2022.2053908.

86 N. Gaspar, X. Ren, C. Smith, J. Grima and K. Evans, Novel honeycombs with auxetic behaviour, *Acta Mater.*, 2005, **53**(8), 2439–2445, DOI: 10.1016/j.actamat.2005.02.006.

87 A. G. Mark, S. Palagi, T. Qiu and P. Fischer, in *Auxetic metamaterial simplifies soft robot design*, *Proc. IEEE Int. Conf. Robot. Autom.*, IEEE, 2016, pp. 4951–4956, DOI: 10.1109/ICRA.2016.7487701.

88 Z. Guo, W. Liu, N. Li and G. Li, Bioinspired hierarchical honeycomb structures: Experiments and modeling, *J. Mech. Phys. Solids*, 2016, **96**, 561–577.

89 E. Dogan, A. Bhusal, B. Cecen and K. Amir, 3D Printing metamaterials towards tissue engineering, *Appl. Mater. Today*, 2020, **20**, 100752, DOI: 10.1016/j.apmt.2020.100752.

90 J. H. Lee, J. P. Singer and E. L. Thomas, Micro-/nanostructured mechanical metamaterials, *Adv. Mater.*, 2012, **24**, 4782–4810, DOI: 10.1002/adma.201201644.

91 A. A. Zadpoor, Mechanical meta-materials, *Mater. Horiz.*, 2016, **3**, 371–381, DOI: 10.1039/c6mh00065g.

92 M. N. Ali, J. J. C. Busfield and I. U. Rehman, Auxetic oesophageal stents: structure and mechanical properties, *J. Mater. Sci. Mater. Med.*, 2014, **25**, 527–553, DOI: 10.1007/s10856-013-5067-2.

93 J. Bauer, L. R. Meza, T. A. Schaedler, R. Schwaiger, X. Zheng and L. Valdevit, Nanolattices: An Emerging Class of Mechanical Metamaterials, *Adv. Mater.*, 2017, **29**, 1701850, DOI: 10.1002/adma.201701850.

94 A. Clausen, F. Wang, J. S. Jensen, O. Sigmund and J. A. Lewis, Topology optimized architectures with Programmable Poisson's ratio over large deformations, *Adv. Mater.*, 2015, **27**, 5523–5527, DOI: 10.1002/adma.201502485.

95 M. Mohsenizadeh, F. Gasbarri, M. Munther, A. Beheshti and K. Davami, Additively manufactured lightweight Metamaterials for energy absorption, *Mater. Des.*, 2018, **139**, 521–530, DOI: 10.1016/j.matdes.2017.11.037.

96 X. Zheng, H. Lee, T. H. Weisgraber, M. Shusteff, J. DeOtte, E. B. Duoss, J. D. Kuntz, M. M. Biener, Q. Ge, J. A. Jackson, S. O. Kucheyev, N. X. Fang and C. M. Spadaccini, Ultralight, ultrastiff mechanical metamaterials, *Science*, 2014, **344**(80), 1373–1377, DOI: 10.1126/science.1252291.

97 T. Bückmann, M. Thiel, M. Kadic, R. Schittny and M. Wegener, An elasto-mechanical unfeelability cloak made of pentamode metamaterials, *Nat. Commun.*, 2014, **5**, 4130, DOI: 10.1038/ncomms5130.

98 S. Hengsbach and A. D. Lantada, Direct laser writing of auxetic structures: present capabilities and challenges, *Smart Mater. Struct.*, 2014, **23**, 085033, DOI: 10.1088/0964-1726/23/8/085033.

99 H. M. A. Kolken and A. A. Zadpoor, Auxetic mechanical metamaterials, *RSC Adv.*, 2017, **7**, 5111–5129, DOI: 10.1039/c6ra27333e.

100 T. Bückmann, N. Stenger, M. Kadic, J. Kaschke, A. Frölich, T. Kennerknecht, C. Eberl, M. Thiel and M. Wegener, Tailored 3D mechanical metamaterials made by dip-in direct-laser-writing optical lithography, *Adv. Mater.*, 2012, **24**, 2710–2714, DOI: 10.1002/adma.201200584.

101 M. Kadic, T. Bückmann, R. Schittny, P. Gumbsch and M. Wegener, Pentamode metamaterials with independently tailored bulk modulus and mass density, *Phys. Rev. Appl.*, 2014, **2**, 054007, DOI: 10.1103/PhysRevApplied.2.054007.

102 T. Frenzel, M. Kadic and M. Wegener, Three-dimensional mechanical metamaterials with a twist, *Science*, 2017, **358**(80), 1072–1074, DOI: 10.1126/science.aao4640.

103 E. Andreassen, B. S. Lazarov and O. Sigmund, Design of manufacturable 3D extremal elastic microstructure, *Mech. Mater.*, 2014, **69**, 1–10, DOI: 10.1016/j.mechmat.2013.09.018.

104 A. J. Jacobsen, J. A. Kolodziejska, R. Doty, K. D. Fink, C. Zhou, C. S. Roper and W. B. Carter, Interconnected self-propagating photopolymer waveguides: an alternative to stereolithography for rapid formation of lattice-based open-cellular materials, *Int. Solid Free. Fabr. Symp.*, 2010, 846–853.

105 L. R. Meza, S. Das and J. R. Greer, Strong, lightweight, and recoverable three-dimensional ceramic nanolattices, *Science*, 2014, **345**(80), 1322–1326, DOI: 10.1126/science.1255908.

106 A. A. Zadpoor, Mechanical performance of additively manufactured meta-biomaterials, *Acta Biomater.*, 2019, **85**, 41–59, DOI: 10.1016/j.actbio.2018.12.038.

107 I. Fernandez-Corbaton, C. Rockstuhl, P. Ziemke, P. Gumbsch, A. Albiez, R. Schwaiger, T. Frenzel, M. Kadic and M. Wegener, New Twists of 3D Chiral Metamaterials, *Adv. Mater.*, 2019, **31**, 1807742.

108 Z. C. Eckel, C. Zhou, J. H. Martin, A. J. Jacobsen, W. B. Carter and T. A. Schaedler, Additive manufacturing of polymer-derived ceramics, *Science*, 2016, **351**(80), 58–62, DOI: 10.1126/science.aad2688.

109 H. Mehboob, F. Tarlochan, A. Mehboob, S.-H. Chang, S. Ramesh, W. Sharuzi Wan Harun and K. Kadirgama, *A novel design, analysis and 3D printing of Ti-6Al-4V alloy bio-inspired porous femoral stem*, Springer, 2020, DOI: 10.1007/s10856-020-06420-7.

110 J. I. Lipton, R. MacCurdy, Z. Manchester, L. Chin, D. Cellucci and D. Rus, *Science*, 2018, **360**, 632.

111 J. Bauer, A. Schroer, R. Schwaiger and O. Kraft, Approaching theoretical strength in glassy carbon nanolattices, *Nat. Mater.*, 2016, **15**, 438–443, DOI: 10.1038/nmat4561.

112 Z. R. Hedayati, A. M. Leeflang and A. A. Zadpoor, Additively manufactured metallic pentamode meta-materials, *Appl. Phys. Lett.*, 2017, **110**, 091905, DOI: 10.1063/1.4977561.

113 Y. Jiang and Q. Wang, Highly stretchable 3D-architected mechanical metamaterials, *Sci. Rep.*, 2016, **6**, 34147, DOI: 10.1038/srep34147.

114 K. Bertoldi, V. Vitelli, J. Christensen and M. Van Hecke, Flexible mechanical metamaterials, *Nat. Rev. Mater.*, 2017, **2**, 1–11, DOI: 10.1038/natrevmats.2017.66.

115 H. Mehboob, F. Tarlochan, A. Mehboob, S.-H. Chang, S. Ramesh, W. S. W. Harun and K. Kadirgama. *A novel design, analysis and 3D printing of Ti-6Al-4V alloy bio-inspired porous femoral stem*, Springer, 2020, DOI: 10.1007/s10856-020-06420-7.

116 R. Wildman, I. Ashcroft and M. Abdi, Design optimization for an additively manufactured automotive component, *Int. J. Powertrains.*, 2017, **7**, 142–161, DOI: **10.1504/ijpt.2018.10009559**.

117 S. Li, H. Hassanin, M. M. Attallah, N. J. E. Adkins and K. Essa, The development of TiNi-based negative Poisson's ratio structure using selective laser melting, *Acta Mater.*, 2016, **105**, 75–83, DOI: **10.1016/j.actamat.2015.12.017**.

118 F. Warmuth, F. Osmanlic, L. Adler, M. A. Lodes and C. Korner, Fabrication and characterisation of a fully auxetic 3D lattice structure via selective electron beam melting, *Smart Mater. Struct.*, 2017, **26**, 025013, DOI: **10.1088/1361-665X/26/2/025013**.

119 J. Schwerdtfeger, F. Schury, M. Stingl, F. Wein, R. F. Singer and C. Korner, Mechanical characterisation of a periodic auxetic structure produced by SEBM, *Phys. Status Solidi B*, 2012, **249**, 1347–1352, DOI: **10.1002/pssb.201084211**.

120 T. Li, X. Hu, Y. Chen and L. Wang, Harnessing out-of-plane deformation to design 3D architected lattice metamaterials with tunable Poisson's ratio, *Sci. Rep.*, 2017, **7**, 8949, DOI: **10.1038/s41598-017-09218-w**.

121 L. Yang, D. Cormier, H. West, O. Harrysson and K. Knowlson, Non-stochastic Ti-6Al-4V foam structures with negative Poisson's ratio, *Mater. Sci. Eng., A*, 2012, **558**, 579–585, DOI: **10.1016/j.msea.2012.08.053**.

122 R. Schittny, T. Bückmann, M. Kadic and M. Wegener, Elastic measurements on macroscopic three-dimensional pentamode metamaterials, *Appl. Phys. Lett.*, 2013, **103**, 231905, DOI: **10.1063/1.4838663**.

123 J. Schwerdtfeger, F. Wein, G. Leugering, R. F. Singer, C. Korner, M. Stingl and F. Schury, Design of auxetic structures via mathematical optimization, *Adv. Mater.*, 2011, **23**, 2650–2654, DOI: **10.1002/adma.201004090**.

124 E. Mazur and I. Shishkovsky, Additively Manufactured Hierarchical Auxetic Mechanical Metamaterials, *Materials*, 2022, **15**, 5600, DOI: **10.3390/ma15165600**.

125 F. Albertini, J. Dirrenberger, C. Sollogoub, T. Maconachie, M. Leary and A. Molotnikov, Experimental and computational analysis of the mechanical properties of composite auxetic lattice structures, *Addit. Manuf.*, 2021, **47**, 102351.

126 A. Ingrole, A. Hao and R. Liang, Design and modeling of auxetic and hybrid honeycomb structures for in-plane property enhancement, *Mater. Des.*, 2017, **117**, 72–83.

127 H. M. A. Kolken, S. Janbaz, S. M. A. Leeflang, K. Lietaert, H. H. Weinans and A. A. Zadpoor, Rationally designed meta-implants: A combination of auxetic and conventional meta-biomaterials, *Mater. Horiz.*, 2017, **5**, 28–35.

128 A. G. Mark, S. Palagi, T. Qiu and P. Fischer, in *Auxetic metamaterial simplifies soft robot design*, *Proc. IEEE Int. Conf. Robot. Autom.*, IEEE, 2016, pp. 4951–4956, DOI: **10.1109/ICRA.2016.7487701**.

129 K. Wang, Y. H. Chang, Y. W. Chen, C. Zhang and B. Wang, Designable dual material auxetic metamaterials using three-dimensional printing, *Mater. Des.*, 2015, **67**, 159–164, DOI: **10.1016/j.matdes.2014.11.033**.

130 M. N. Ali, J. J. C. Busfield and I. U. Rehman, Auxetic oesophageal stents: structure and mechanical properties, *J. Mater. Sci.: Mater. Med.*, 2014, **25**, 527–553, DOI: **10.1007/s10856-013-5067-2**.

131 A. Clausen, F. Wang, J. S. Jensen, O. Sigmund and J. A. Lewis, Topology optimized architectures with Programmable Poisson's ratio over large deformations, *Adv. Mater.*, 2015, **27**, 5523–5527, DOI: **10.1002/adma.201502485**.

132 S. Vyavahare, S. Teraiya and S. Kumar, An Experimental Study of Influence of Gradient Parameters on Compressive Strength, Stiffness, and Specific Energy Absorption (SEA) of Auxetic Structures Fabricated by FDM, *Oxidative Stress Heart Dis.*, 2021, 305–318.

133 D. Mocerino, M. R. Ricciardi, V. Antonucci and I. Papa, Fused Deposition Modelling of Polymeric Auxetic Structures: A Review, *Polymers*, 2023, **15**, 1008, DOI: **10.3390/polym15041008**.

134 S. Yuan, F. Shen, J. Bai, C. K. Chua, J. Wei and K. Zhou, 3D soft auxetic lattice structures fabricated by selective laser sintering: TPU powder evaluation and process optimization, *Mater. Des.*, 2017, **120**, 317–327, DOI: **10.1016/j.matdes.2017.01.098**.

135 H. Yazdani Sarvestani, A. H. Akbarzadeh, A. Mirbolghasemi and K. Hermenean, 3D printed meta-sandwich structures: failure mechanism, energy absorption and multi-hit capability, *Mater. Des.*, 2018, **160**, 179–193, DOI: **10.1016/j.matdes.2018.08.061**.

136 P. Madhu Balan, A. Johnney Mertens and M. V. A. Raju Bahubalendruni, Auxetic mechanical metamaterials and their futuristic developments: A state-of-art review, *Mater. Today Commun.*, 2023, **34**, 105285.

137 Z. Li, L. Wang, X. Geng, W. Chen and B. Han, Complex uncertainty-oriented robust topology optimization for multiple mechanical metamaterials based on double-layer mesh, *Comp. Meth. Appl Mech Eng.*, 2024, **419**, 116589, DOI: **10.1016/j.cma.2023.116589**.